Journal of Medicinal Chemistry



Article

# Binding modes of reverse fosmidomycin analogs towards the antimalarial target IspC

Sarah Konzuch, Tomonobu Umeda, Jana Held, Saskia Hähn, Karin Brücher, Claudia Lienau, Christoph Behrendt, Tobias Gräwert, Adelbert Bacher, Boris Illarionov, Markus Fischer, Benjamin Mordmüller, Nobutaka Tanaka, and Thomas Kurz

*J. Med. Chem.*, **Just Accepted Manuscript** • DOI: 10.1021/jm500850y • Publication Date (Web): 25 Sep 2014

# Binding modes of reverse fosmidomycin analogs towards the antimalarial target IspC

*Sarah Konzuch,[†] Tomonobu Umeda,[∥] Jana Held,[#] Saskia Hähn,[†] Karin Brücher,[†] Claudia Lienau,[†] Christoph T. Behrendt,[†] Tobias Gräwert,[§] Adelbert Bacher,[§] Boris Illarionov,[§] Markus Fischer,[§] Benjamin Mordmüller,[#,▽] Nobutada Tanaka,[∥] and Thomas Kurz*[*,†]*

[†]Institut für Pharmazeutische und Medizinische Chemie, Heinrich Heine Universität, Universitätsstr. 1, 40225 Düsseldorf, Germany; [∥]School of Pharmacy, Showa University, Tokyo 142-8555, Japan; [#]Institut für Tropenmedizin, Eberhard Karls Universität Tübingen, Wilhelmstr. 27, 72074 Tübingen, Germany; [§]Hamburg School of Food Science, Universität Hamburg, Grindelallee 117, 20146 Hamburg, Germany; and [▽]Medical Research Unit, Albert Schweitzer Hospital, Lambaréné, Gabon

**RECEIVED DATE (to be automatically inserted after your manuscript is accepted if required according to the journal that you are submitting your paper to)**

CORRESPONDING AUTHOR FOOTNOTE [†]Institut für Pharmazeutische und Medizinische Chemie, Heinrich-Heine-Universität, Universitätsstr. 1, 40225 Düsseldorf, Germany. Phone: (+49)21181-14985, Fax -13847, E-mail: thomas.kurz@uni-duesseldorf.de.

ABSTRACT 1-Deoxy-D-xylulose 5-phosphate reductoisomerase of *Plasmodium falciparum* (*Pf*IspC, *Pf*Dxr), believed to be the rate-limiting enzyme of the non-mevalonate pathway of isoprenoid biosynthesis (MEP pathway), is a clinically validated antimalarial target. The enzyme is efficiently inhibited by the natural product fosmidomycin. In order to gain new insights into the structure activity relationships of reverse fosmidomycin analogs, several reverse analogs of fosmidomycin were synthesized and biologically evaluated. The 4-methoxyphenyl substituted derivative **2c** showed potent inhibition of *Pf*IspC as well as of *P. falciparum* growth and was more than one order of magnitude more active than fosmidomycin. The binding modes of three new derivatives in complex with *Pf*IspC, NADPH and $Mg^{2+}$ were determined by X-ray structure analysis. Notably, *Pf*IspC selectively binds the *S*-enantiomers of the study compounds.

## INTRODUCTION

Despite considerable research activities, malaria remains one of the most widespread and life-threatening infectious disease of the world. Because of new drug combinations and improved vector control the mortality rate has been reduced significantly since 2004, when the number of deaths peaked at 1.8 million. However, the current situation is still alarming and global efforts are required to accomplish the goal of malaria elimination. Despite increased funding and public awareness the WHO reported 207 million estimated malaria cases and 627,000 estimated deaths in 2012. [1]

Malaria control relies heavily on early diagnosis followed by antimalarial chemotherapy to prevent death as well as potentially fatal complications such as severe anemia and coma. Malaria therapy is compromised by current and emerging parasite resistance towards nearly all established antimalarials.[2] In most countries with endemic malaria, fixed-dose artemisinin-based combination therapies have now become first-line treatments and parenteral artesunate has become the treatment of choice for severe malaria. However, cases of reduced parasite sensitivity towards artemisinin derivatives have been reported.[3] Thus, antimalarial drugs with new modes of action are urgently needed.[4,5]

A promising approach for the discovery of antimalarials is the inhibition of the non-mevalonate isoprenoid biosynthesis (MEP pathway).[6,7] The MEP pathway is essential in the *Plasmodium ssp.* causing malaria (and also in some other pathogenic protozoa and many pathogenic bacteria including *Mycobacterium tuberculosis* and *Pseudomonas aeruginosa*), but is absent in mammalians.[2,8] Hence, drugs directed at enzymes of the non-mevalonate pathway should be exempt from target-related toxicity.

1-Deoxy-D-xylulose 5-phosphate reductoisomerase (IspC, Dxr) catalyzes the first committed reaction step of the non-mevalonate pathway (Fig. 1) and has been validated as a malaria target by clinical studies using fosmidomycin, an antibiotic from *Streptomyces lavendulae*.[4,9,10,11,12,13]

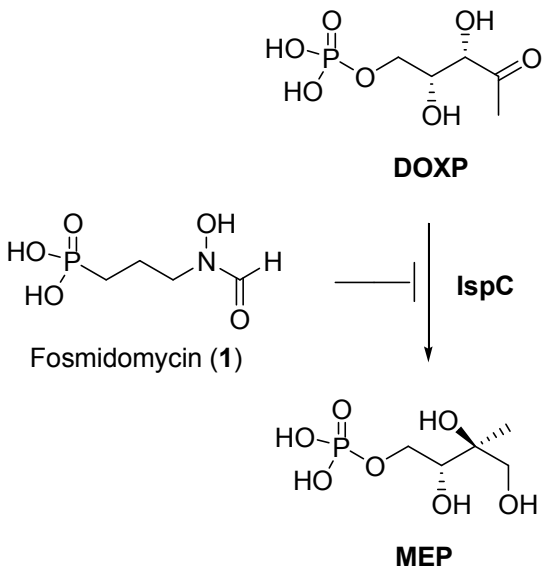


**Figure 1.** Inhibition of IspC.

Although crystal structures of *Pf*IspC in the presence and absence of inhibitors (fosmidomycin, FR900098, an α-pyridyl-substitited FR900098 analog and a reverse fosmidomycin β-thia isostere) were recently reported, the rational design of improved fosmidomycin analogs is still difficult, because *Pf*IspC undergoes a complex conformational transition when binding the substrate, 1-deoxyxylulose 5-phosphate (DOXP) or one of the inhibitors studied.[14-16] Earlier studies mostly focused on *Ec*IspC and *Mt*IspC crystal structures as the basis for the rational design of (*Pf)*IspC inhibitors.[17-28]

In order to gain new insights regarding the structure activity relationships of reverse fosmidomycin analogs, we have modified several key regions of lead structures **A, B** (Figure 2). Specifically, we address the substitution pattern of the α-phenyl-substituent (first reverse compounds with donor substituents $CH_3$, $OCH_3$) (**2a-f**), the length (**4**) and the chemical functionality (β-oxa isosters **3a-b**) of the spacer as well as the nature of the metal ion chelating group (**6**, **7**). Moreover we report the first crystal structures of *Pf*IspC in complex with reverse α-aryl-substituted carba- and oxa-analogs (**2a**, **2c**, **3a**).

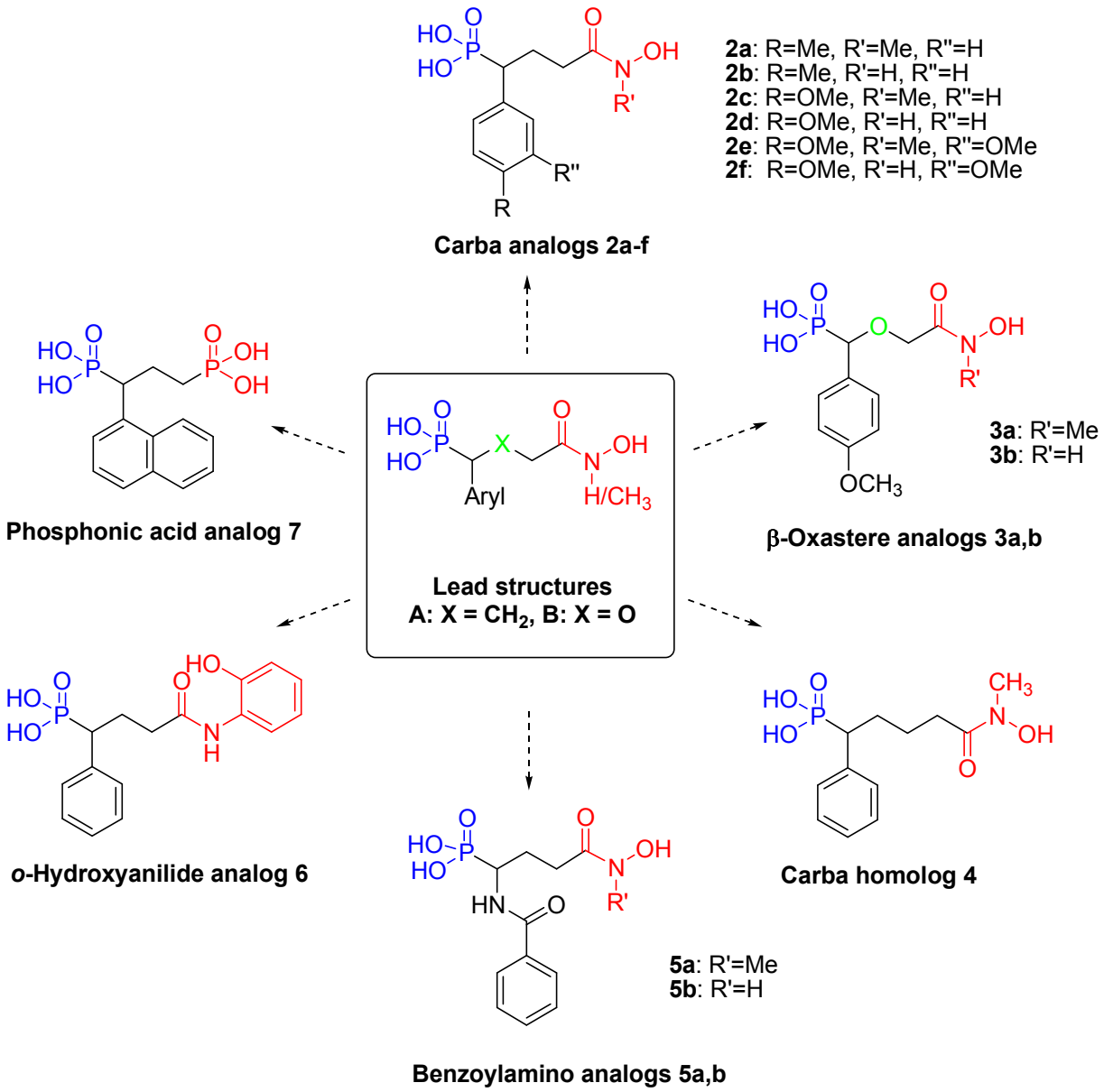


**Figure 2**. Lead structures and target compounds.

RESULTS

**Chemical synthesis.**

*Carba-analogs and β-oxa isosteres.* Carba-analogs (**2a-d**) and β-oxa isosteres (**3a-b**) of fosmidomycin (Figure 2) were prepared according to previously published procedures (supporting information Scheme S1).[29,30] Carba analogs **2e-f** were synthesized by a modified procedure starting from diethyl 3,4-dimethoxybenzylphosphonate **8a**.[31] Briefly, C-alkylation of **8a** with 2-(2-bromoethyl)-1,3-dioxolane in the presence of *n*-BuLi afforded 1,3-dioxolane **9a**. Hydrolysis of the 1,3-dioxolane moiety of **9a** by treatment with water and Dowex 50WX8 provided aldehyde **10a**,[32] which was subsequently oxidized to carboxylic acid **11a**. Coupling reactions of **11a** with *O*-benzyl-hydroxylamine or *N*-methyl-*O*-benzylhydroxylamine furnished *O*-benzyl-protected hydroxamic acids **12a** and **14a**.[33] Dealkylation of diethyl phosphonates (**12a**, **14a)** with bromotrimethylsilane provided the corresponding phosphonic acids, which were directly converted into dibenzylphosphonates **13a** and **15a** using *N*,*N*'-dicyclohexylcarbodiimide (DCC) and benzyl alcohol. Finally, catalytic hydrogenation afforded hydroxamic acids **2e** and **2f** as white solids (Scheme 1).

**Scheme 1.** Synthesis of target compounds **2e** and **2f**[a]

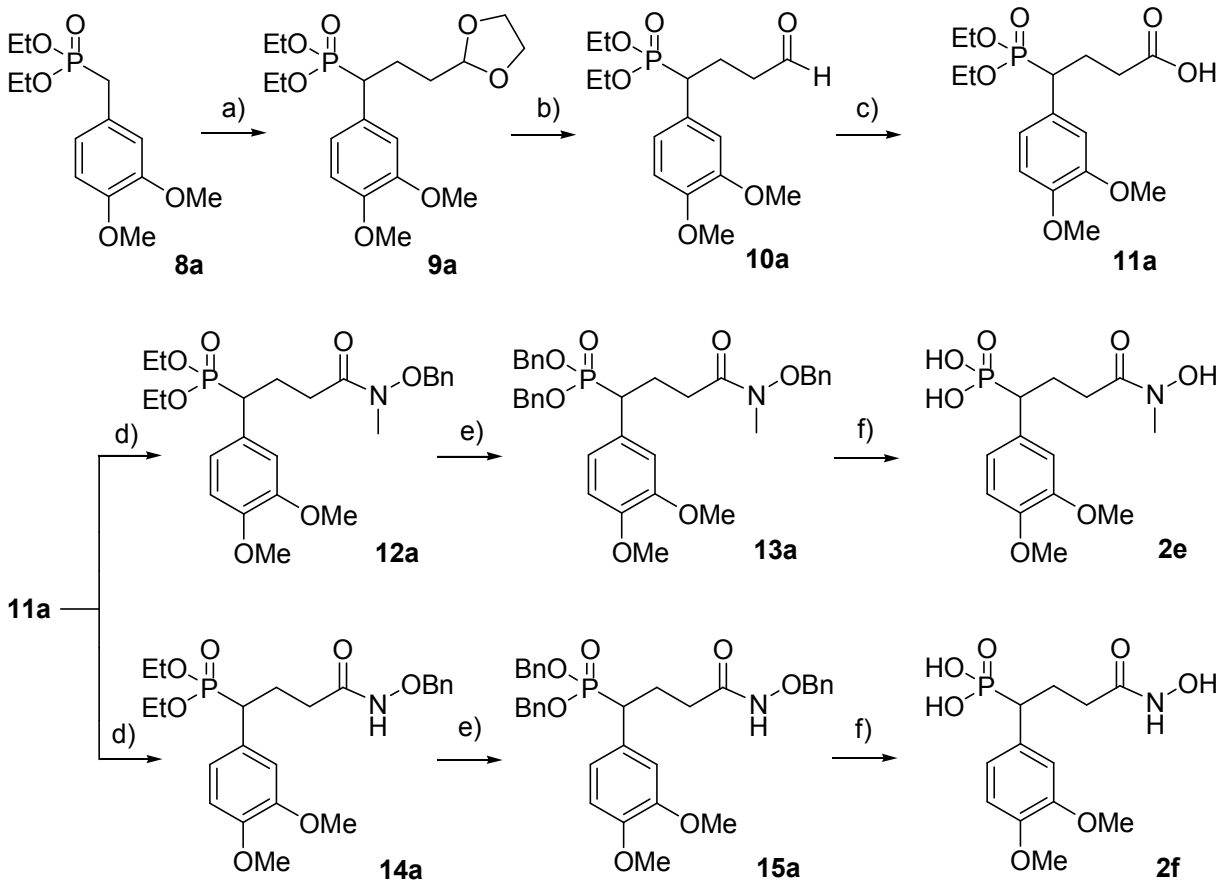


[a]Reagents and conditions: a) *n*-BuLi, 2-(2-bromoethyl)-1,3-dioxolane, toluene, -78 °C, 12 h, 56 %; b) Dowex 50WX8, acetone/$H_2O$, rt, 24 h, 70 %; c) $H_2O_2$, $SeO_2$, THF, 4 h, reflux, 90 %; d) isobutyl chloroformate, NMM, BnONHR (R = H, Me), THF, -20 °C, 10 min → rt, 30 min, 50 % (**12a**), 65 % (**14a**); e) 1. TMSBr, $CH_2Cl_2$, rt, 24 h; 2. THF/$H_2O$, rt, 1 h, 3. DCC, BnOH, benzene, 80 °C, 4h, 18 % (**13a**), 30 % (**15a**); f) $H_2$, Pd-C, MeOH, rt, 3 h, 95 % (**2e**), 98 % (**2f**).

*Carba homolog 4*. Alkylation of phosphonate **8b**[29,34] with 2-(3-bromopropyl)-1,3-dioxolane[35] in the presence of *n*-BuLi afforded the protected intermediate **9b**. Acidic hydrolysis of the 1,3-dioxolane moiety provided aldehyde **10b**, which was directly oxidized to carboxylic acid **11b**. Coupling of the crude carboxylic acid **11b** with *O*-benzyl-*N*-methylhydroxylamine utilizing 1,1´-carbonyldiimidazole (CDI) as coupling agent provided *O*-benzyl-protected hydroxamic acid **12b** in 74 % yield and good purity. Cleavage of phosphonic ester **12b** with bromotrimethylsilane yielded phosphonic acid **16b**. Finally, catalytic hydrogenation of crude **16b** afforded the target hydroxamate **4** in 92 % yield (Scheme 2).

**Scheme 2.** Synthesis of compound **4**[a]

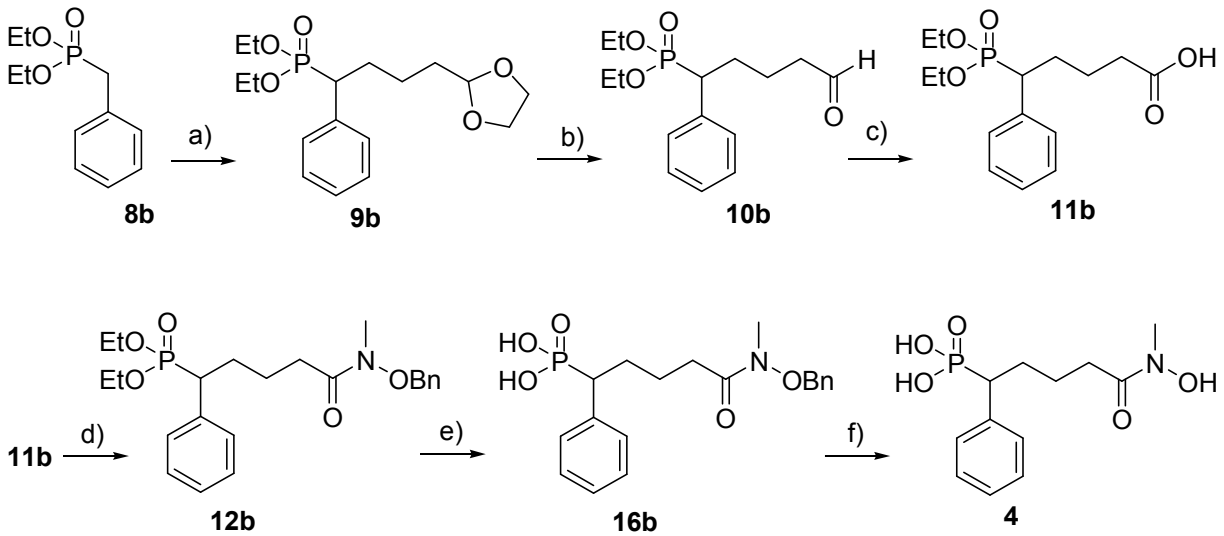


[a]Reagents and conditions: a) *n*-BuLi, 2-(3-bromopropyl)-1,3-dioxolane, toluene, -78 °C, 12 h, 77 %; b) 2 M HCl, acetone, 50 °C, 3 h, 77 %; c) $SeO_2$, $H_2O_2$, THF, 65 °C, 4 h, 66 %; d) CDI, BnONHMe, $CH_2Cl_2$, rt, 12 h, 85 %; e) 1. TMSBr, $CH_2Cl_2$, rt, 24 h; 2. THF/$H_2O$, rt, 1 h, 81 % (crude yield); f) $H_2$, Pd-C, MeOH, rt, 1 h, 92 %.

*Benzoylamino analogs* ***5a-b***. Treatment of α-aminophosphonate **25**[36] with benzoyl chloride and TEA afforded benzamide **26** in 59 % yield. Conversion of **26** into hydroxamic acids **27**, **28** was accomplished by hydroxylaminolysis.[37] Finally, cleavage of the diethylphosphonate moiety using bromotrimethylsilane yielded derivatives **5a-b** (Scheme 3).

**Scheme 3.** *Synthesis of benzoylamino analogs 5a-b*[a]

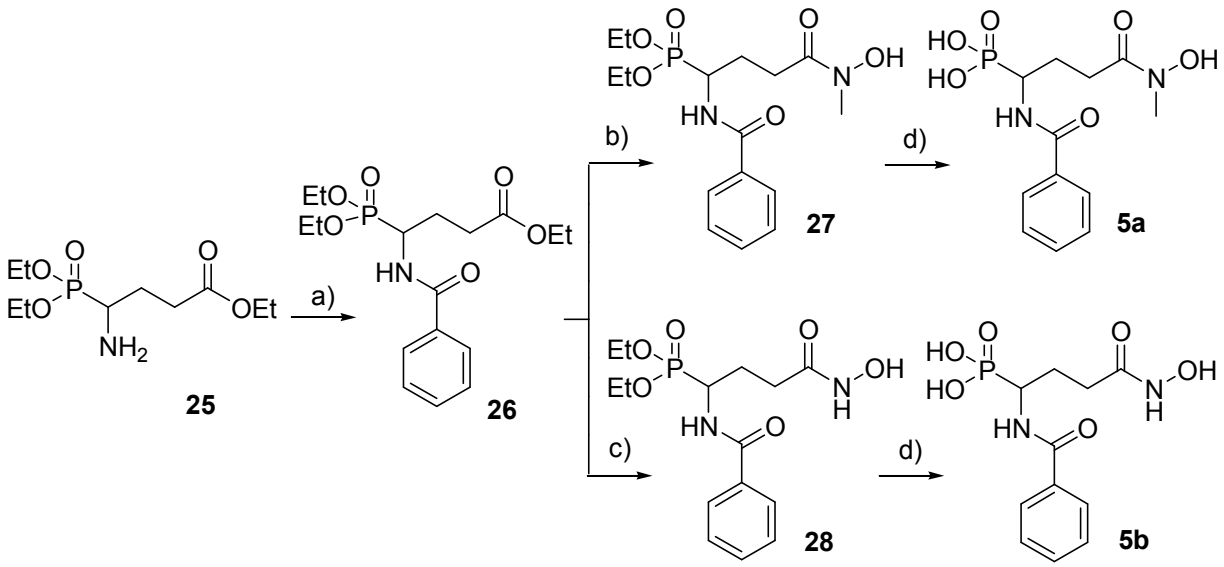


[a]Reagents and conditions: a) benzoyl chloride, TEA, $CH_2Cl_2$, rt, 12 h, 59 %; b) *N*-methylhydroxylamine hydrochloride, NaOH, MeOH, 0 °C → rt, 12 h, 34 %; c) hydroxylamine hydrochloride, NaOH, MeOH, 0 °C → rt, 30 min, 53 %; d) 1. TMSBr, $CH_2Cl_2$, rt, 24 h; 2. THF/$H_2O$, rt, 1 h, 70 % (**5a**), 44 % (**5b**).

*o-Hydroxyanilide* ***6***. Carboxylic acid **29**[29] was converted into the corresponding acyl chloride which was subsequently reacted with 2-benzyloxyaniline to provide anilide **30**. Catalytic hydrogenation of **30** yielded the protected *o*-hydroxyanilide **31**. Finally, cleavage of the phosphonic acid ester group using bromotrimethylsilane led to target compound **6** with an *o*-hydroxy-anilide moiety as a potential metal ion binding group (Scheme 4).

**Scheme 4.** Synthesis of *o*-hydroxyanilide **6**[a]

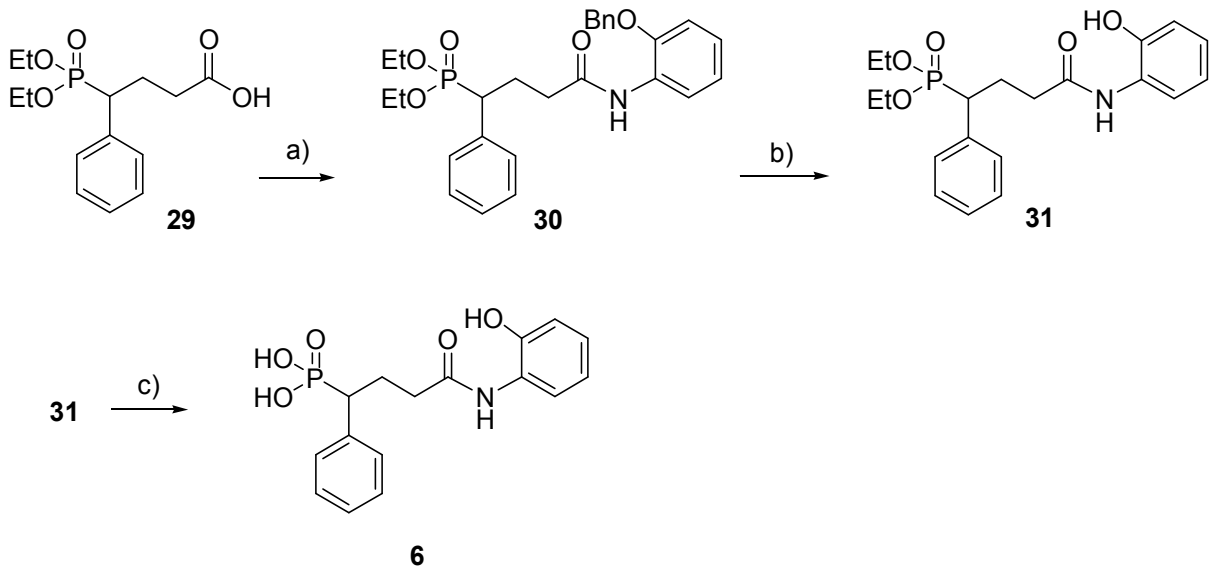


[a]Reagents and conditions: a) 1. $(COCl)_2$, DMF, toluene, rt, 1 h; 2. 2-benzyloxyaniline, pyridine, $CH_2Cl_2$, rt, 12 h, 70 %; b) $H_2$, Pd-C (10 %), MeOH, 2 bar, rt, 3 h, 83 %; c) 1) TMSBr, $CH_2Cl_2$, rt, 24 h; 2) THF/$H_2O$ (~100:1), rt, 1 h, 52 %.

*Synthesis of bisphosphonate 7. C*-Alkylation of phosphonate **8e**[17,38] with excess of 1,2-dibromoethane in the presence of *n*-butyllithium afforded bromide **32**. Michaelis-Arbuzov reaction of **32** with triethyl phosphite provided phosphonic ester **33** (Scheme 5). Transesterification of **33** yielded the completely *O*-Bn-protected derivative **34**, which was finally deprotected by catalytic hydrogenation.

**Scheme 5.** Synthesis of target compound **7**[a]

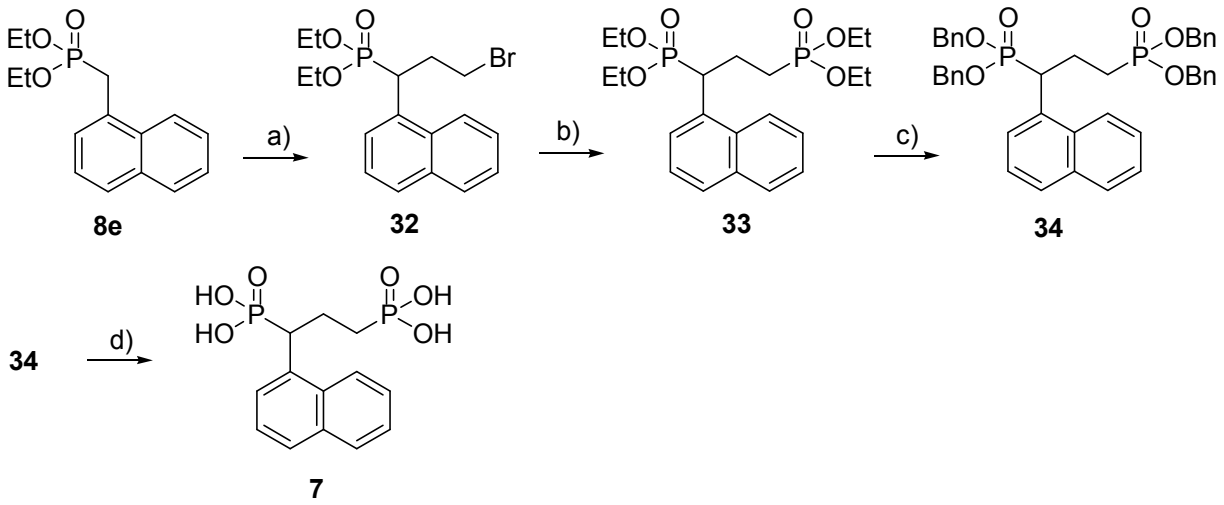


[a]Reagents and conditions: a) *n*-BuLi, 1,2-dibromoethane (4 eq), toluene, -78 °C, 12 h, 60 %; b) triethyl phosphite, 160 °C, 1 h, 180 °C 12 h, 97 %; c) 1. TMSBr, $CH_2Cl_2$, rt, 24 h; 2. THF/$H_2O$, rt, 1 h; 3. DCC, BnOH, benzene, 80 °C, 4 h, 16 % (3 steps); d) $H_2$, Pd-C, MeOH, 1 bar, rt, 3 h, 97 %.

**Biological evaluation.**

The study compounds were screened against IspC from *P. falciparum* (*Pf*IspC), *Escherichia coli* (*Ec*IspC) and *Mycobacterium tuberculosis* (*Mt*IspC) using a photometric assay that has been described earlier.[29] $IC_{50}$ values were determined by nonlinear regression analysis using the program package Dynafit.[39] Curve shapes were closely similar in all cases. Typical examples are shown in Fig. 3 (top).

We also measured the growth-inhibitory effect of the study compounds against asexual stage *P. falciparum* malaria parasites. Specifically, we used one chloroquine-sensitive and two multi-drug resistant *P. falciparum* strains of different geographic origin (3D7, Dd2 and FCR3). Parasite growth was monitored by measuring expression of *P. falciparum* histidine rich protein 2 by enzyme-linked immunosorbent assay exactly as described previously.[40] Reverse carba and oxa analogs (**2**, **3**) are potent *P. falciparum* growth inhibitors. Several new derivatives displayed $IC_{50}$ values in the double digit nanomolare range (Table 1). Typical examples (same compounds as in Fig. 3, top) are shown as the bottom part of Fig. 3. It should be noted that the parasite assay curves are typically descending faster than the cognate enzyme inhibition curves.

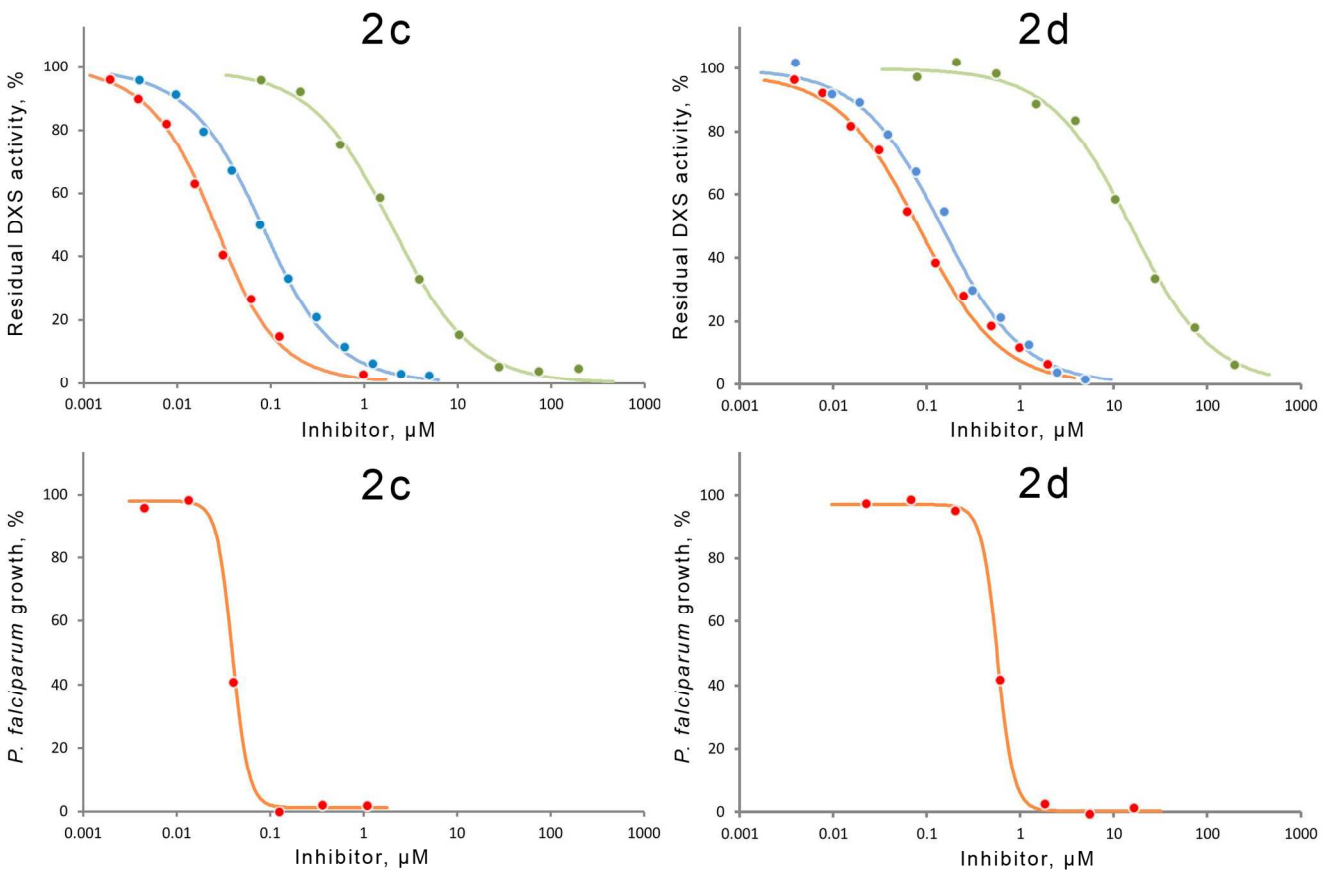


**Figure 3.** Top, inhibition of IspC orthologs (*Pf*IspC, red; *Ec*IspC, blue; *Mt*IspC, green). Bottom, inhibiton of *P. falciparum* blood stages; left, compound **2c**, right, compound **2d**.).

Numerical data for all compounds studied are summarized in Table 1.

**Table 1.** Enzyme inhibition and *in vitro* antiplasmodial activity.

| | Ar | R‘ | *Pf*IspC[a] $IC_{50}$ [µM] | *Ec*IspC[a] $IC_{50}$ [µM] | *Mt*IspC[a] $IC_{50}$ [µM] | *Pf*3D7[b] $IC_{50}$ [µM] | *Pf*Dd2[b,f] $IC_{50}$ [µM] | *Pf*FCR3[b,f] $IC_{50}$ [µM] |
|---|---|---|---|---|---|---|---|---|
| **1** | | | 0.16 ± 0.02[c] | 0.22 ± 0.01[d] | 0.23 ± 0.02[e] | 0.88[d] | 0.81[d] | n.d. |
| **2a** | 4-Me-Ph | Me | 0.01 ± 0.002 | 0.29 ± 0.02 | 1.8 ± 0.1 | 0.21 | 0.25 | 0.38 |
| **2b** | 4-Me-Ph | H | 0.19 | 0.70 | 11 | 2.6 | 2.8 | n.d. |

| | | | | | | | | |
|---|---|---|---|---|---|---|---|---|
| | | | ± 0.01 | ± 0.1 | ± 1 | | | |
| **2c** | 4-MeO-Ph | Me | 0.02 | 0.07 | 2.0 | 0.10 | 0.30 | 0.57 |
| | | | ± 0.002 | ± 0.003 | ± 0.1 | | | |
| **2d** | 4-MeO-Ph | H | 0.08 | 0.14 | 15 | 1.7 | 3.6 | n.d. |
| | | | ± 0.008 | ± 0.01 | ± 1.0 | | | |
| **2e** | 3,4-MeO-Ph | Me | 0.06 | 0.32 | 29 | 0.29 | 1.2 | n.d. |
| | | | ± 0.006 | ± 0.01 | ± 1.0 | | | |
| **2f** | 3,4-MeO-Ph | H | 0.13 | 1.5 | 163 | 6.8 | 8.1 | n.d. |
| | | | ± 0.02 | ± 0.1 | ± 34 | | | |
| **3a** | 4-MeO-Ph | Me | 0.05 | 0.45 | 2.8 | 0.31 | 1.1 | 0.41 |
| | | | ± 0.004 | ± 0.04 | ± 2.0 | | | |
| **3b** | 4-MeO-Ph | H | 2.2 | 17 | 352 | > 50 | n.d. | n.d. |
| | | | ± 0.1 | ± 1.0 | ± 29 | | | |
| **4** | Ph | - | 2.1 | 4.3 | 429 | > 50 | n.d. | n.d. |
| | | | ± 0.1 | ± 0.1 | ± 29 | | | |
| **5a** | NH-CO-Ph | Me | 9.1 | 11 | 238 | > 50 | n.d. | n.d. |
| | | | ± 1.3 | ± 0 | ± 21 | | | |
| **5b** | NH-CO-Ph | H | > 1000 | 741 | > 1000 | > 50 | n.d. | n.d. |
| | | | | ± 94 | | | | |
| **6** | Ph | - | > 300 | > 500 | > 500 | > 50 | n.d. | n.d. |
| **7** | 1-Naphthyl | - | > 300 | > 500 | > 500 | > 50 | n.d. | n.d. |

[a]Enzyme assay. Values were calculated from eight or more data points. In general two or three independent determinations have been performed.[39,41] [b]*In vitro* assay. Values are the mean of two duplicate determinations. [c]$IC_{50}$ value according to ref 16. [d]$IC_{50}$ value according to ref 15. [e]$IC_{50}$ value according to ref 13. [f]n.d., not determined. Details regarding the structure of the compounds can be found in Figure 2.

The inhibitors under study are more active against IspC from *P. falciparum* than against the bacterial orthologs (Fig. S1, Fig. 4A). Notably, the inhibition of the *M. tuberculosis* enzyme exceeds that of the Plasmodium enzyme by about two orders of magnitude. This is well in line with earlier observations

indicating that α-aryl analogs of fosmidomycin are more potent inhibitors for the plasmodial enzyme than for the bacterial enzymes that have been included in comparative studies.[14,30] In contrast to the differential activities of the study compounds, authentic fosmidomycin showed similar inhibition of the IspC from *P. falciparum* and the bacterial enzymes (Table 1, Fig. S1).

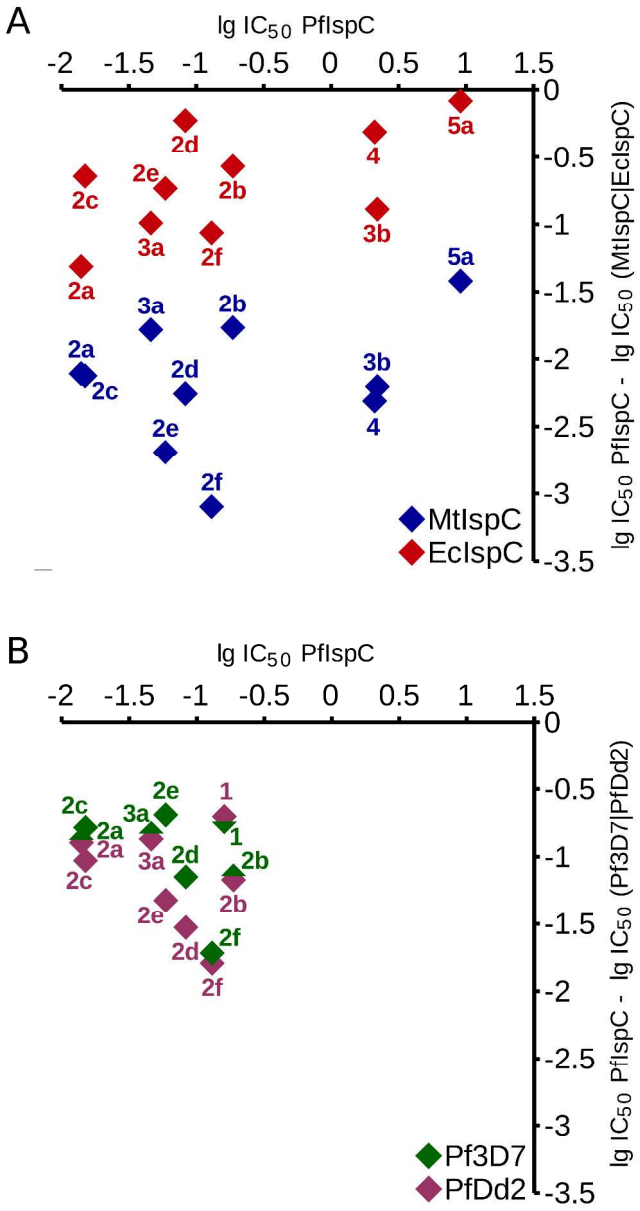


**Figure 4.** Top, ortholog specificity of IspC inhibition; the ordinate reflects the $IC_{50}$ ratio of eubacterial IspCs and *Pf*IspC; the inhibitory potency of the study compounds for *Pf*IspC exceeds that for *Mt*IspC by about two orders of magnitude (blue diamonds) and that for *Ec*IspC by close to one order of magnitude. Bottom, activity ($IC_{50}$ values) against blood stages of two different *P. falciparum* strains versus *in vitro*

inhibition of *Pf*IspC ($IC_{50}$ values); both test strains show similar responses; the sensitivity of the isolated enzyme exceeds that of the growing parasite by about one order of magnitude.

According to Fig. 4B, the $IC_{50}$ values of the study compounds for the enzymatic target, *Pf*IspC, are lower, by approximately one order of magnitude, than the $IC_{50}$ values observed in asexual blood stages. On the other hand, due to the different curve shapes illustrated in Fig. 3, the inhibitor concentrations required for 90 % inhibition are similar in the enzyme and parasite assays.

The most active compounds in Table 1 (carba analogs **2a**, **2c**) had $IC_{50}$ values in the low nanomolecular range for the plasmodial enzyme, and exceed the inhibitory effect of authentic fosmidomycin to a significant degree (Table 1). Extending the chain length (**4**) caused the inhibitory activity to drop by several orders of magnitude. The replacement of the $Me^{2+}$ binding hydroxamic acid pharmacophore by other potentially metal ion binding groups e.g. an *o*-hydroxyanilide moiety (**6**) and a phosphonic acid group (**7**) led to complete loss of inhibitory activity .

**Crystal structure analysis.**

Cocrystallization of *Pf*IspC with NADPH, $Mg^{2+}$ and reverse fosmidomycin analogs (**2a**, **2c**, and **3a**) afforded crystals with space group $P2_1$ for **2a** and **2c** complexes and $P3_121$ for the **3a** complex (diffraction to resolutions of 2.25, 1.97, and 2.35 Å (Table S1)). Structures were solved by molecular replacement using the structure of IspC in complex with NADPH, $Mg^{2+}$ and fosmidomycin (PDB accession code 3AU9) as search model.

The asymmetric units of crystals of **2a** and **2c** complexes comprise two IspC subunits, whereas that of the **3a-**complex comprises one subunit. The subunit in the asymmetric unit of the crystal containing **3a** is related by a crystallographic 2-fold axis to form a homodimer. The structural differences between two subunits in the asymmetric unit of **2a** and **2c** complexes are described in the “Structure determination”

section of the Supporting Information. For simplicity, the following description refers primarily to subunit B of the **2c** complex.

The active site structure of the quaternary complexes reported in this paper show significant differences from those of previously published quaternary (fosmidomycin- or FR900098-containing) complexes of *Pf*IspC,[15] although tertiary (three-domain structure) and quaternary (homo dimer) structures are conserved (Fig. 5a). The **2c** molecule is located in the active site cavity (Figure 5a).

The α-aryl substituent has van der Waals contacts with active site residues; specifically, the side chains of Ser270, Cys338, and Pro358 are well ordered, whereas Trp296 and Met298 showed higher temperature factors (Figure 5b). In addition, an intra-molecular interaction is observed between the *N*-methyl group and the aromatic ring of **2c**. The *N*-methyl group has a contact with the side chain of Met360. A comparison of the binding mode of **2c** with that of fosmidomycin reveals that in a closed conformation, as observed with Trp296 in the fosmidomycin complex, Trp296 would crash with the α-aryl substituent of **2c** (Figure 5c). In fact, the flexible loop region (residues 291-299) in the **2c** complex adopts a relatively open conformation. As compared with the fosmidomycin complex, the flexible loop of the **2c** complex is rather disordered (poorer electron density and higher B-factors). Therefore, the cause of the tight binding of **2c** to *Pf*IspC appears to be different from that of fosmidomycin to *Pf*IspC, but similar to that of the 3,4-difluorophenyl analog[17] to *Ec*IspC. Recently, we have reported the crystal structure of *Pf*IspC in complex with an α-phenyl substituted reverse thia analog of fosmidomycin.[14] The molecular interaction between **2c** and *Pf*IspC is similar to that between the thia analog and *Pf*IspC, however, significant conformational differences are observed for the flexible loop region.

The phosphonate group of **2c** forms a tight hydrogen-bond network with the main chain NH and side chain OH of Ser270, the side chain of Asn311, two water molecules, and the side chain of Ser306 (Figure 6a). In the fosmidomycin:IspC complex, the side chain of His293 is involved in the hydrogen-bond network instead of Ser306 (Figures 5c and 6b).

The present crystal structures are the first examples of quaternary complexes of IspC with reverse carba and oxa analogs. The reverse-hydroxamate group coordinates an $Mg^{2+}$ ion that is bound by residues Asp231, Glu233, and Glu315. Thus, the $Mg^{2+}$ ion has distorted trigonal bipyramidal geometry. This metal coordination geometry is consistent with that of the hydroxamate group of fosmidomycin observed in the previously published quaternary complexes of *Pf*IspC,[14,15] but different from that of the reverse-hydroxamate group observed in the ternary complex of *E. coli* IspC crystallized in the absence of NADPH.[17] The octahedral sixfold metal ion coordination observed in the ternary complex of *Ec*IspC (two inhibitor atoms, three protein ligands, and a water molecule) is unlikely to occur in the quaternary complex of *Pf*IspC because the water molecule would crash with the nicotinamide ring of NADPH. Comparing a possible hydrogen-bond network of the **2c** complex and the fosmidomycin (or FR900098) complex (Figures 6a and 6b), the metal coordination abilities and hydrogen-bond network with surrounding residues are essentially equivalent. This is consistent with the similar inhibitory activities of fosmidomycin and a reverse-hydroxamate analog reported by Kuntz.[42]

To examine differences in inhibitor-induced conformation changes dependent on the type of inhibitors, the crystal structures of *Pf*IspC complexed with **2a** (α-Ph-$CH_3$), **2c** (α-Ph-$OCH_3$), and fosmidomycin were compared (Figure 5d). It is interesting that the degree of loop closure is related to the size of the bound inhibitor. This knowledge concerning the induced-fit mechanism of *Pf*IspC will be useful for designing new inhibitors. In addition, the flexible loop of **2a** complex is also rather disordered as compared with that of the fosmidomycin complex. Thus, the primary factor of the tight binding of **2a** and **2c** to *Pf*IspC as compared with that of fosmidomycin which lacks the aryl group would be van der Waals interactions between the α-aryl group and the core of the active site rather than the flexible loop (Figures 6a and 6b).

In the present crystal structure analyses, we also determined a *Pf*IspC-NADPH-$Mg^{2+}$**-3a** quaternary complex. The **3a** complex is quite similar to the **2c** complex. The current structure-activity relationship data (Table 1) show that β-oxa compounds have somewhat lower inhibitory activities than their carba

counterparts. This is explained by structural comparison of the **2c** complex with the fosmidomycin complex (Figure 5c). Due to the presence of a bulky substituent at the α-position, the methylene spacer of **2c** adopts a different conformation as compared with that of fosmidomycin. The methylene spacer of **3a** adopts a conformation that is equivalent with that of **2c**. In the fosmidomycin complex, the β-position of the carbon spacer is accommodated in a hydrophilic environment where it interacts with the side chains of Glu233, Lys312 and a water molecule, whereas the β-position of inhibitors **2c** and **3a** is accommodated in a hydrophobic environment and interacts with the Cβ of Ser306 and the Cε of Met298. Therefore, the β-oxygen of α-substituted oxa derivatives may have somewhat unfavorable interactions with the active site as compared with their carba counterparts.

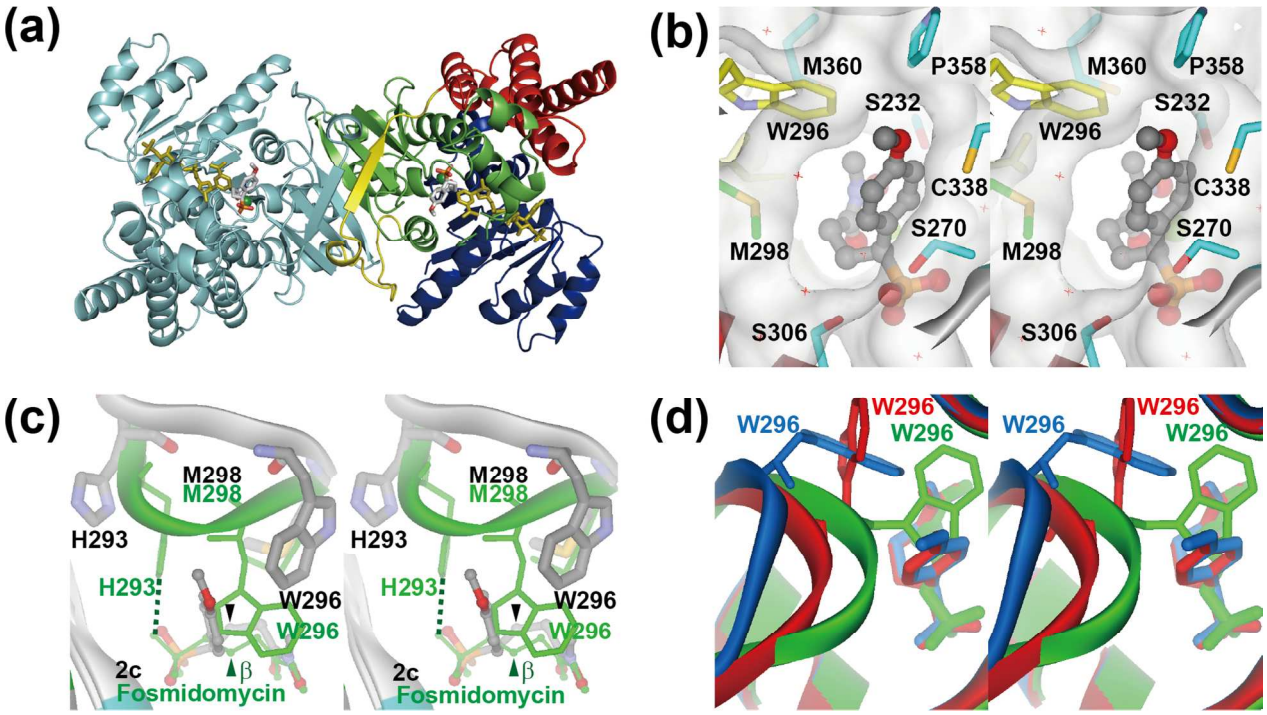


**Figure 5.** Crystal structure analyses of *Pf*IspC. (a) Overall structure of the **2c**-containing quaternary complex of *Pf*IspC. One subunit is colored by domains: the NADPH-binding, catalytic, linker, and *C*-terminal domains are depicted in blue, green, yellow, and red, respectively. The other subunit is colored cyan. The bound **2c** and NADPH molecules are shown as sticks. The bound $Mg^{2+}$ ions are shown as spheres. (b) Close-up view of the active site with bound **2c**. The side chains surrounding the α-aryl substituent are shown and the carbon atoms are colored by their B-factors: cyan (15~25 $Å^2$), green

(25~35 Å$^2$), and yellow (35~45 Å$^2$). Note that the side chains belonging to the flexible loop, Trp296 and Met298, show higher B-factors. (c) A structural comparison of the binding mode of **2c** (grey) and that of fosmidomycin (green) (PDB code 3AU9) in the active site of *Pf*IspC. The β-positions of the methylene spacer of the bound inhibitors are marked by arrowheads. The bound inhibitor molecules are shown as ball-and-stick models. (d) A comparison of the induced-fit movements of the flexible loop (residues 291-299) of *Pf*IspC. The **2a**-, **2c**-, and fosmidomycin-bound quaternary complexes of *Pf*IspC are shown in blue, red, and green, respectively.

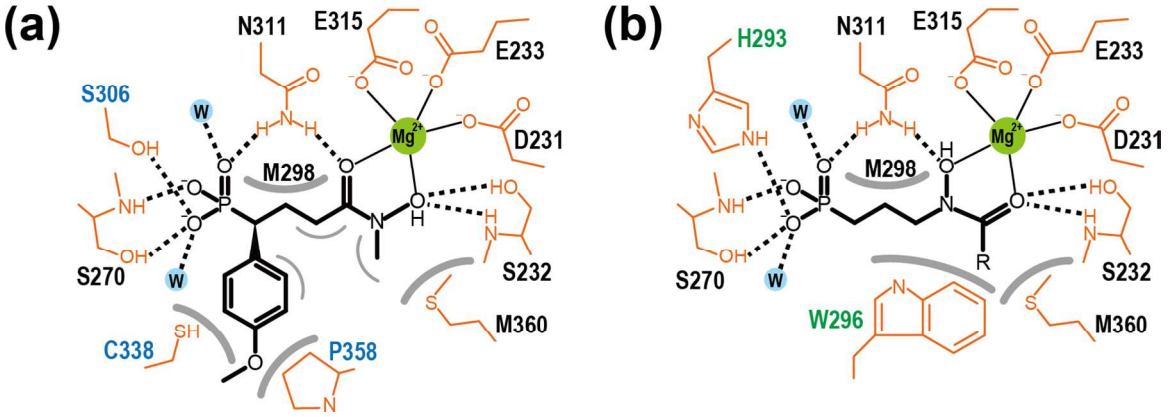


**Figure 6.** Schematic overview of the interactions of inhibitors in the active site of *Pf*IspC. Metal coordination (2.0~2.1 Å) and possible hydrogen bonds (2.7~3.1 Å) are shown as solid and dashed lines, respectively. Intra- and intermolecular van der Waals contacts are shown as thin and thick gray arcs, respectively. (a) **2c** complex. Residues uniquely involved in direct interactions with the bound inhibitor in the **2c** complex are shown in blue. (b) Fosmidomycin (R = H) / FR900098 (R=$CH_3$) complex. Residues uniquely involved in direct interactions with the bound inhibitor in the fosmidomycin / FR900098 complex are shown in green.

## DISCUSSION

Using IspC orthologs from the protozoon, *P. falciparum*, and two eubacteria, we found that the shapes of the inhibition curves are all closely similar (cf. Fig. 3). There is no sign whatsoever of positive or negative cooperativity.

Whereas the natural product fosmidomycin inhibits IspC orthologs from *P. falciparum*, *E. coli* and *M. tuberculosis* with similar potency, our data confirm earlier observations that α-aryl derivatives are significantly more potent for the *Plasmodium* enzyme than for the eubacterial orthologs. With *Pf*IspC, the most potent α-aryl derivatives that have been described have $IC_{50}$ values in the low nanomolar range. In terms of their $IC_{50}$, the most potent α-aryl derivatives exceed the inhibitory potential of the natural compound, fosmidomycin, by more than an order of magnitude. A potential explanation for the higher inhibitory activities of α-aryl derivatives against *Pf*IspC is that the difference in structural flexibilities of IspC molecules, i.e. difference in inter-domain and active-site loop flexibilities, may affect the inhibitory activities of bulky inhibitors. Another explanation is that the side chain of Cys338 in *Pf*IspC would have a favorable van der Waals contact with the α-aryl group of the inhibitors (Figure 5b) as compared with structurally corresponding serine residue in *Ec*IspC and *Mt*IspC.

The $IC_{50}$ values observed with the *Plasmodium* enzyme and with multiplying asexual *P. falciparum* blood stages are remarkably well correlated; the $IC_{50}$ values observed for the parasite blood stage are typically one to two orders larger than the $IC_{50}$ values observed with *Pf*IspC *in vitro*. Since the inhibitors must pass through numerous membrane barriers (the erythrocyte membrane, the parasitophorous vacuole membrane, the cell membrane of the parasite and the four membranes of the apicoplast) in order to reach their enzyme target in the living parasite, this may not be particularly surprising. Importantly, however, the inhibition curves observed with the isolated enzyme and the growing parasite are remarkably different in so far as the latter are much steeper. Whereas the $IC_{50}$ values for the isolated enzyme and the growing parasite are offset by one to two units on the log scale, the difference of inhibitory efficacy between enzyme assay and parasite assay essentially vanishes at higher inhibitor concentrations, as a result of the different curve shapes. We can only speculate with regard to the causes of the curve shapes. However, there is no reason to expect a simple parallelism between IspC inhibition and *Plasmodium* proliferation. Quite possibly, growth retardation may only become relevant when the enzyme activity is depressed below a certain threshold value; such a situation could translate into a steep

slope for the parasite growth curve. Of course, under the aspect of drug development, the minimal inhibitory concentration is far more relevant than the $IC_{50}$, and the steeper shape of the parasite growth curves should turn out in favor of a potential therapeutic application of modified fosmidomycin derivatives.

Recently, we could show that *Pf*IspC has a high degree of enantioselectivity for an α-arylated β-thia analog of fosmidomycin (inhibition by the *S*-enantiomer is at least three orders of magnitude stronger as compared with the *R*-enantiomer). Pure enantiomers of the compounds reported in this paper have unfortunately not been obtained as yet. However, the *S*-configuration of the bound inhibitors is the preferred interpretation in this study (Fig. S2) in agreement with previous studies for α-aryl substituted fosmidomycin derivatives.[14,17,26,27] The clear omit map at 1.97 Å resolution for **2c** (Fig. S2(b)) does not look like a mixture of both enantiomers. The X-ray structure data strongly suggest that the *S*-enantiomers of the compounds in this study bind preferentially to the active site of *Pf*IspC. This will hopefully translate into an increase of apparent inhibitory power of the study compounds, once the preparation of pure enantiomers is achieved.

## CONCLUSION

We report on kinetic and crystallographic proof for the mechanism of action of a new series of reverse analogs of fosmidomycin. By modifying different key regions of the lead structure we provided new insights into the structure-activity relationships of reverse fosmidomycin derivatives. The 4-methoxy-phenyl substituted derivative **2c** showed potent inhibition of *Pf*IspC as well as of *P. falciparum* growth and exceeds the inhibitor activity of fosmidomycin by more than one order of magnitude more. Crystallographic studies also demonstrated that *Pf*IspC binds selectively the *S*-enantiomers of α-aryl substituted carba and oxa analogs of fosmidomycin. Our results provide helpful information for the design of novel IspC inhibitors.

EXPERIMENTAL SECTION

All solvents and chemicals were used as purchased without further purification. The progress of all reactions was monitored on Merck precoated silica gel plates (with fluorescence indicator $UV_{254}$) using ethyl acetate / *n*-hexane as solvent system. Column chromatography was performed with Fluka silica gel 60 (230-400 mesh ASTM) with the solvent mixtures specified in the corresponding experiment. Spots were visualized by irradiation with ultraviolet light (254 nm). Melting points (mp) were taken in open capillaries using a Mettler FP 5 melting-point apparatus or a Stuart melting point apparatus SMP11 and are uncorrected. Proton ($^{1}H$) and carbon ($^{13}C$) NMR spectra were recorded using Bruker Avance 500 (500.13 MHz for $^{1}H$; 125.76 MHz for $^{13}C$) or Bruker Avance 600 (600.22 MHz for $^{1}H$; 150.93 MHz for $^{13}C$) spectrometers using [D6]DMSO and $CDCl_3$ as solvents. Chemical shifts are given in parts per million (ppm, δ relative to residual solvent peak for $^{1}H$ and $^{13}C$ or to external tetramethylsilane). Elemental analysis was performed with a Perkin Elmer PE 2400 CHN elemental analyser or a vario MICRO cube elemental analyser (Elementar Analysensysteme GmbH, Hanau, Germany). If necessary, the purity was determined by high performance liquid chromatography (HPLC). HPLC was performed in analogy to a previously reported procedure.[43] The Instrument was an Elite LaChrom system (Hitachi L-2130 pump and L-2400 UV-detector) or a Varian ProStar HPLC System (Varian ProStar 210 pump, Varian ProStar 320 UV-detector and Varian ProStar 410 autosampler). The column was a Phenomenex Luna C-18(2) 5 µm particle (250 mm × 4.6 mm), supported by Phenomenex Security Guard Cartridge Kit C18 (4.0 mm × 3.0 mm). Purity of all final compounds was 95 % or higher, except compound **6** (purity 92.2 %).

**Experimental Data for Compounds.** Experimental data are listed below for selected compounds **9a-15a**, **2e** and **2f**.

**General procedure for the synthesis of dioxolanes (9a-d).**[29] At a temperature of -78 °C, a 1.6 M solution of *n*-butyllithium in *n*-hexane (1.1 eq, 44 mmol, 27.5 mL) was slowly added to a solution of the

respective diethyl arylmethylphosphonate **8a-d** (1 eq, 40 mmol) in dry toluene (50 mL) via a syringe under positive pressure of dry nitrogen. After stirring for 1 h, 2-(2-bromoethyl)-1,3-dioxolane or 2-(3-bromopropyl)-1,3-dioxolane (1 eq, 40 mmol) was added in one portion. The reaction mixture was allowed to warm up to room temperature and stirred overnight. Ethyl acetate (50 mL) was added and the solution was washed three times with an aqueous solution of $NH_4Cl$ (10 %, 50 mL). The organic layer was dried over $Na_2SO_4$, filtered and concentrated under reduced pressure. The crude oil was purified by column chromatography on silica gel using ethyl acetate / *n*-hexane (1:1) as the eluent to give compounds **9a-d** as colorless oils.

**Diethyl 1-(3,4-dimethoxyphenyl)-3-(1,3-dioxolan-2-yl)propylphosphonate (9a).** Colorless oil (13.05 g, 84 %); $^1$H NMR (500.13 MHz, [D$_6$]DMSO): δ = 1.05 (t, *J* = 7.0 Hz, 3H, $CH_2CH_3$), 1.21 (t, *J* = 7.0 Hz, 3H, $CH_2CH_3$), 1.32-1.39 (m, 1H, $CH_2$), 1.43-1.50 (m, 1H, $CH_2$), 1.78-1.88 (m, 1H, $CH_2$), 1.96-2.05 (m, 1H, $CH_2$), 3.09 (ddd, *J* = 21.8, 11.4, 4.0 Hz, 1H, PC*H*), 3.68-3.76 (m, 9H, $OCH_3$, $CHOOCH_2$), 3.80-3.87 (m, 3H, $CH_2CH_3$, $CHOOCH_2$), 3.92-4.01 (m, 2H, $CH_2CH_3$), 4.74 (t, *J* = 4.6 Hz, 1H, C*H*OO), 6.81-6.83 (m, 1H), 6.89-6.91 (m, 2H) ppm; $^{13}$C NMR (125.76 MHz, [D$_6$]DMSO): δ = 16.0 (d, $^3J_{C\text{-}P}$ = 5.5 Hz, $CH_2CH_3$), 16.2 (d, $^3J_{C\text{-}P}$ = 5.5 Hz, $CH_2CH_3$), 24.0 ($CH_2CH_2$), 31.1 (d, $^2J_{C\text{-}P}$ = 14.7 Hz, $CHCH_2$), 41.9 (d, $^1J_{C\text{-}P}$ = 136.8 Hz, P*C*H), 55.3 ($OCH_3$), 55.4 ($OCH_3$), 61.0 (d, $^2J_{C\text{-}P}$ = 7.1 Hz, $CH_2CH_3$), 61.5 (d, $^2J_{C\text{-}P}$ = 7.0 Hz, $CH_2CH_3$), 64.1 ($CHOOCH_2$), 64.2 ($CHOOCH_2$), 103.0 (*C*HOO), 111.6, 112.9 (d, $^3J_{C\text{-}P}$ = 6.4 Hz), 121.1 (d, $^2J_{C\text{-}P}$ = 7.4 Hz), 128.3 (d, $^3J_{C\text{-}P}$ = 6.6 Hz), 147.7, 148.3 ppm; anal. calcd. for $C_{18}H_{29}O_7P$: C 55.66, H 7.53, found: C 55.29, H 7.89.

**Diethyl 1-(3,4-dimethoxyphenyl)-4-oxobutylphosphonate (10a).**[32] Dowex 50WX8 (3mL) was added to a solution of dioxolane **9a** (14.5 mmol, 5.63 g) in water/acetone (10:1, 5 mL), . After stirring at room temperature for 48 h, the solution was filtered. The filtrate was concentrated, diluted with saturated aqueous NaCl solution and extracted three times with ethyl acetate (100 mL). The organic layer was dried over $Na_2SO_4$ and concentrated under reduced pressure. Column chromatography on silica gel using ethyl acetate gave compound **10a** as a colorless oil (3.25 g, 65 %); 1H NMR (500.13 MHz,

[$D_6$]DMSO): δ = 1.05 (t, *J* = 7.0 Hz, 3H, $CH_2CH_3$), 1.22 (t, *J* = 7.0 Hz, 3H, $CH_2CH_3$), 1.95-2.05 (m, 1H, $CH_2$), 2.15-2.23 (m, 1H, $CH_2$), 2.25-2.39 (m, 2H, $CH_2$), 3.09 (ddd, *J* = 21.8, 11.3, 4.2 Hz, 1H, PC*H*), 3.72 (s, 3H, $OCH_3$), 3.73 (s, 3H, $OCH_3$), 3.80-3.90 (m, 2H, $CH_2CH_3$), 3.93-4.03 (m, 2H, $CH_2CH_3$), 6.79-6.82 (m, 1H), 6.88-6.91 (m, 2H), 9.55 (s, 1H, C*H*O); $^{13}$C NMR (125.76 MHz, [$D_6$]DMSO): δ = 16.1 (d, $^3J_{C\text{-}P}$ = 5.6 Hz, $CH_2CH_3$), 16.2 (d, $^3J_{C\text{-}P}$ = 5.5 Hz, $CH_2CH_3$), 22.3 ($CH_2CH_2$), 40.9 (d, $^2J_{C\text{-}P}$ = 14.8 Hz, $CHCH_2$), 41.5 (d, $^1J_{C\text{-}P}$ = 137.0 Hz, P*C*H), 55.3 ($OCH_3$), 55.4 ($OCH_3$), 61.2 (d, $^2J_{C\text{-}P}$ = 7.2 Hz, $CH_2CH_3$), 61.6 (d, $^2J_{C\text{-}P}$ = 7.0 Hz, $CH_2CH_3$), 111.6, 112.7 (d, $^3J_{C\text{-}P}$ = 6.3 Hz), 121.2 (d, $^2J_{C\text{-}P}$ = 7.3 Hz), 127.8 (d, $^3J_{C\text{-}P}$ = 6.6 Hz), 147.8, 148.4, 202.6 (*C*HO); anal. calcd. for $C_{16}H_{25}O_6P$: C 55.81, H 7.32, found: C 55.79, H 7.39.

**General procedure for the synthesis of carboxylic acids (11a-d).**[29] To a solution of the respective aldehyde **10a-d** (1 eq, 5 mmol) in THF (7.5 mL), $H_2O_2$ (1.1 mL of a 30 % solution) and $SeO_2$ (0.5 eq, 2.5 mmol, 0.28 g) were added. The solution was refluxed for 4 h and the reaction mixture was concentrated under reduced pressure. Ethyl acetate (50 mL) was added to the remaining oil and the resulting solution was washed three times with 1 M hydrochloric acid (10 mL). After drying over $Na_2SO_4$, the organic solvent was removed under reduced pressure. The crude products **11c-d** were treated with diethyl ether (20 mL) and stored at 7 °C to give compounds **11c-d** as white solids. Pure compounds **11a** and **11b** were obtained without further purification.

**4-(Diethoxyphosphoryl)-4-(3,4-dimethoxyphenyl)butanoic acid (11a).** Yellow resin (1.58 g, 88 %); $^1$H NMR (500.13 MHz, [$D_6$]DMSO): δ = 1.06 (t, *J* = 7.0 Hz, 3H, $CH_2CH_3$), 1.22 (t, *J* = 7.0 Hz, 3H, $CH_2CH_3$), 1.91-2.01 (m, 1H, $CH_2$), 2.06-2.10 (m, 2H, $CH_2$), 2.13-2.19 (m, 1H, $CH_2$), 3.10 (ddd, *J* = 21.8, 11.1, 4.0 Hz, 1H, PC*H*), 3.73 (s, 3H, $OCH_3$), 3.74 (s, 3H, $OCH_3$), 3.78-3.89 (m, 1H, $CH_2CH_3$), 3.93-4.07 (m, 3H, $CH_2CH_3$), 6.80-6.81 (m, 1H), 6.87 (s, 1H), 6.91 (d, *J* = 8.3 Hz, 1H), 12.10 (s, 1H, COO*H*); $^{13}$C NMR (125.76 MHz, [$D_6$]DMSO): δ = 16.0 (d, $^3J_{C\text{-}P}$ = 5.5 Hz, $CH_2CH_3$), 16.2 (d, $^3J_{C\text{-}P}$ = 5.5 Hz, $CH_2CH_3$), 25.0 ($CH_2CH_2$), 41.3 (d, $^2J_{C\text{-}P}$ = 15.4 Hz, $CHCH_2$), 41.5 (d, $^1J_{C\text{-}P}$ = 137.7 Hz, P*C*H), 55.3 ($OCH_3$), 55.4 ($OCH_3$), 61.1 (d, $^2J_{C\text{-}P}$ = 7.1 Hz, $CH_2CH_3$), 61.6 (d, $^2J_{C\text{-}P}$ = 6.8 Hz, $CH_2CH_3$), 111.6, 112.7

(d, $^3J_{C\text{-}P}$ = 6.3 Hz), 121.2 (d, $^2J_{C\text{-}P}$ = 7.3 Hz), 127.9 (d, $^3J_{C\text{-}P}$ = 6.7 Hz), 147.8, 148.4, 173.6 (*C*OOH); HPLC analysis: retention time = 1.84 min; peak area: 93.3 %. Eluent A: 5 mM $NH_4OAc$ solution; eluent B: $CH_3CN$, isocratic (1:1) over 20 min at a flow rate of 1 mL $min^{-1}$.

**General procedure for the synthesis of *O*-Bn-protected hydroxamic acids (12a, 14a).**[33] To a solution of the carboxylic acid **11a** (1 eq, 5 mmol, 1.80 g) in dry THF (50 mL) *N*-methylmorpholin (NMM) (1.1 eq, 5.5 mmol, 506 mg) was added. The solution was cooled down to -20 °C and isobutyl chloroformate (1.1 eq, 5.5 mmol, 751 mg) was added. After 10 min, the appropriate hydroxylamine (1 eq, 5 mmol) was added dropwise. The reaction mixture was warmed up to room temperature overnight. The precipitated NMM-hydrochloride was filtered off and the filtrate was concentrated under reduced pressure. The residue was dissolved in $H_2O$ / ethyl acetate and the aqueous layer was extracted three times with ethyl acetate (50 mL). The organic layers were combined and washed twice with a saturated aqueous solution of $NaHCO_3$ (10 mL), dried over $Na_2SO_4$, filtered and concentrated under reduced pressure. The crude product was purified by column chromatography on silica gel using ethyl acetate/*n*-hexane (1:1) as the eluent to give compounds **12a** and **14a** as yellow oils.

**Diethyl 4-[benzyloxy(methyl)amino]-1-(3,4-dimethoxyphenyl)-4-oxobutylphosphonate (12a).** Yellow oil (1.53 g, 64 %); $^1$H NMR (600.22 MHz, [D6]DMSO): δ = 1.05 (t, *J* = 7.0 Hz, 3H, $CH_2CH_3$), 1.21 (t, *J* = 7.0 Hz, 3H, $CH_2CH_3$), 1.90-1.97 (m, 1H, $CH_2$), 2.13-2.28 (m, 3H, $CH_2$), 3.10-3.14 (m, 4H, PC*H*, $NCH_3$), 3.71-3.77 (m, 7H, $OCH_3$, $CH_2CH_3$), 3.80-3.86 (m, 1H, $CH_2CH_3$), 3.94-4.01 (m, 2H, $CH_2CH_3$), 4.66 (dd, *J* = 22.5, 9.9 Hz, 2H, $PhCH_2$), 6.82 (d, *J* = 8.2 Hz,1H), 6.88 (s, 1H), 6.92 (d, *J* = 8.2 Hz), 7.17-7.18 (m, 2H), 7.30-7.36 (m, 3H) ppm; $^{13}$C NMR (150.93 MHz, [D6]DMSO): δ = 16.0 (d, $^3J_{C\text{-}P}$ = 5.5 Hz, $CH_2CH_3$), 16.2 (d, $^3J_{C\text{-}P}$ = 5.5 Hz, $CH_2CH_3$), 24.6 ($CH_2CH_2$), 29.2 (d, $^2J_{C\text{-}P}$ = 16.2 Hz, $CHCH_2$), 32.6 ($NCH_3$), 41.7 (d, $^1J_{C\text{-}P}$ = 137.2 Hz, PCH), 55.3 ($OCH_3$), 55.4 ($OCH_3$), 61.1 (d, $^2J_{C\text{-}P}$ = 7.0 Hz, $CH_2CH_3$), 61.5 (d, $^2J_{C\text{-}P}$ = 6.9 Hz, $CH_2CH_3$), 75.1 ($PhCH_2$), 111.6, 112.8 (d, $^3J_{C\text{-}P}$ = 6.4 Hz), 121.2 (d, $^2J_{C\text{-}P}$ = 7.4 Hz), 128.1 (d, $^3J_{C\text{-}P}$ = 6.7 Hz), 128.3, 128.6, 129.3, 147.8 (d, $^5J_{C\text{-}P}$ = 2.3 Hz), 148.4 (d, $^4J_{C\text{-}P}$

= 1.7 Hz), 173.0 (C=O) ppm; anal. calcd. for $C_{24}H_{34}NO_7P$: C 60.12, H 7.15, N 2.92, found: C 60.37, H 7.31, N 2.65.

**Diethyl 4-(benzyloxyamino)-1-(3,4-dimethoxyphenyl)-4-oxobutylphosphonate (14a).** Yellow oil (1.07 g, 46 %); $^1$H NMR (500.13 MHz, [D6]DMSO): δ = 1.05 (t, *J* = 7.0 Hz, 3H, $CH_2CH_3$), 1.22 (t, *J* = 7.0 Hz, 3H, $CH_2CH_3$), 1.82 (t, *J* = 7.5 Hz, 2H, $CH_2$), 1.91-1.99 (m, 1H,$CH_2$), 2.12-2.21 (m, 1H, $CH_2$), 3.05 (ddd, *J* = 21.8, 11.3, 3.5 Hz, 1H, PC*H*), 3.72 (s, 3H, $OCH_3$), 3.73 (s, 3H, $OCH_3$), 3.79-3.87 (m, 2H, $CH_2CH_3$), 3.93-4.00 (m, 2H, $CH_2CH_3$), 4.74 (s, 2H, $PhCH_2$), 6.78 (d, *J* = 8.2 Hz, 1H), 6.84 (s, 1H), 6.89 (d, *J* = 8.3 Hz, 1H), 10.51 (s, 0.1H, *E*-isomer, O*H*), 10.87 (s, 0.9H, Z-isomer, O*H*) ppm; $^{13}$C NMR (125.76 MHz, [D6]DMSO): δ = 16.1 (d, $^3J_{C\text{-}P}$ = 5.6 Hz, $CH_2CH_3$), 16.2 (d, $^3J_{C\text{-}P}$ = 5.4 Hz, $CH_2CH_3$), 25.3 ($CH_2CH_2$), 29.9 ($CHCH_2$), 41.7 (d, $^1J_{C\text{-}P}$ = 136.7 Hz, P*C*H), 55.3 ($OCH_3$), 55.4 ($OCH_3$), 61.2 (d, $^2J_{C\text{-}P}$ = 6.9 Hz, $CH_2CH_3$), 61.6 (d, $^2J_{C\text{-}P}$ = 6.7 Hz, $CH_2CH_3$), 76.6 ($PhCH_2$), 111.5, 112.7 (d, $^3J_{C\text{-}P}$ = 6.3 Hz), 121.2 (d, $^3J_{C\text{-}P}$ = 7.0 Hz), 127.8 (d, $^2J_{C\text{-}P}$ = 6.7 Hz), 128.1, 128.2, 128.6, 136.0, 147.7 (d, $^5J_{C\text{-}P}$ = 2.8 Hz), 148.3, 168.5 (*C*=O) ppm; anal. calcd. for $C_{23}H_{32}NO_7P$: C 59.35, H 6.93, N 3.01, found: C 59.08, H 7.22, N 2.82.

**General procedure for the synthesis of tri-*O*-benzyl protected phosphonohydroxamic acids (15a,c,d, 13a, 24, 34).**[29] To a solution of the respective phosphonic acid diethyl ester (**14a**,**c**,**d**, **12a**, **23**, **33**) (1 eq, 3 mmol) in dry $CH_2Cl_2$ (10 mL), trimethylsilyl bromide (5 eq, 15 mmol, 1.99 mL in case of compounds **15a**,**c**,**d**, **13a**, **24**; 10 eq, 30 mmol, 3.98 mL in case of compound **34**) was added at 0 °C. After 1 h, the solution was allowed to warm up to room temperature and stirred for 23 h. The solvent was removed under reduced pressure. The residue was dissolved in THF (10 mL) and treated with water (0.1 mL). After 30 min, the solvent was evaporated and the residue was dried under reduced pressure overnight. The residue was dissolved in benzene (20 mL). 2-Benzyl-1,3-dicyclohexyl-isourea (2 eq, 6 mmol, 1.89 g in case of compounds **15a**,**c**,**d**, **13a**, **24**; 4 eq, 12 mmol, 3.78 g in case of compound **34**) was added. The mixture was refluxed for 6 h. After cooling to room temperature, ethyl acetate (30 mL) was added, solid 1,3-dicyclohexyl-urea was filtered off and the solvent was removed under reduced

pressure. Column chromatography on silica gel using ethyl acetate provided compounds **15a**,**c**,**d**, **13a**, **24** and **34**.

**Dibenzyl 4-[benzyloxy(methyl)amino]-1-(3,4-dimethoxyphenyl)-4-oxobutylphosphonate (13a).** Yellow oil (550 mg; 30 %); 1H NMR (500.13 MHz, [D6]DMSO): δ = 1.99-2.03 (m, 1H, C*H₂*), 2.20-2.28 (m, 3H, C*H₂*), 3.09 (s, 3H, NC*H₃*), 3.26-3.32 (m, 1H, PC*H*), 3.61 (s, 3H, OC*H₃*), 3.73 (s, 3H, OC*H₃*), 4.64 (dd, *J* = 24.6, 9.9 Hz, 2H, PhC*H₂*), 4.76 (dd, *J* = 12.0, 7.8 Hz, 1H, PhC*H₂*), 4.85 (dd, *J* = 12.0, 6.8 Hz, 1H, PhC*H₂*), 4.96 (dd, *J* = 12.0, 7.1 Hz, 1H, PhC*H₂*), 5.02 (dd, *J* = 12.0, 8.5 Hz, 1H, PhC*H₂*), 6.83-6.84 (m, 1H), 6.87 (s, 1H), 6.91 (d, *J* = 8.3 Hz), 7.17-7.18 (m, 4H), 7.29-7.37 (m, 11H) ppm; $^{13}$C NMR (125.76 MHz, [D6]DMSO): δ = 24.4 ($CH_2CH_2$), 29.2 (d, $^2J_{C\text{-}P}$ = 16.4 Hz, $CHCH_2$), 32.6 ($NCH_3$), 41.8 (d, $^1J_{C\text{-}P}$ = 136.3 Hz, P*C*H), 55.2 ($OCH_3$), 55.4 ($OCH_3$), 66.5 (d, $^2J_{C\text{-}P}$ = 6.9 Hz, $CH_2CH_3$), 66.8 (d, $^2J_{C\text{-}P}$ = 6.5 Hz, $CH_2CH_3$), 75.1 ($PhCH_2$), 111.7, 112.8 (d, $^3J_{C\text{-}P}$ = 6.2 Hz), 121.2 (d, $^3J_{C\text{-}P}$ = 7.4 Hz), 127.4, 127.6, 127.7 (d, $^2J_{C\text{-}P}$ = 7.2 Hz), 127.9, 128.0, 128.2, 128.2, 128.3, 128.6, 129.3, 134.3, 136.5 (d, $^3J_{C\text{-}P}$ = 6.1 Hz), 136.6 (d, $^3J_{C\text{-}P}$ = 6.4 Hz), 147.9 (d, $^5J_{C\text{-}P}$ = 2.3 Hz), 148.5 (d, $^4J_{C\text{-}P}$ = 1.5 Hz), 172.9 (*C*=O) ppm; anal. calcd. for $C_{34}H_{38}NO_7P$: C 67.65, H 6.35, N 2.32, found: C 67.43, H 6.20, N 2.28.

**Dibenzyl 4-(benzyloxyamino)-1-(3,4-dimethoxyphenyl)-4-oxobutylphosphonate (15a).** Yellow oil (248 mg; 14 %); $^1$H NMR (500.13 MHz, [D6]DMSO): δ = 1.83-1.86 (m, 2H, C*H₂*), 1.97-2.06 (m, 1H, C*H₂*), 2.24-2.28 (m, 1H, C*H₂*), 3.23 (ddd, *J* = 22.0, 11.4, 3.2 Hz, 1H, PC*H*), 3.61 (s, 3H, OC*H₃*), 3.73 (s, 3H, OC*H₃*), 4.73-4.77 (m, 3H, PhC*H₂*), 4.83-4.87 (m, 1H, PhC*H₂*), 4.94-5.04 (m, 2H, PhC*H₂*), 6.80 (d, *J* = 8.2 Hz, 1H), 6.83 (s, 1H), 6.89 (d, *J* = 8.2 Hz, 1H), 7.17-7.19 (m, 2H), 7.30-7.37 (m, 12H), 10.51 (s, 0.1H, *E*-isomer, O*H*), 10.87 (s, 0.9H, *Z*-isomer, O*H*) ppm; $^{13}$C NMR (125.76 MHz, [D6]DMSO): δ = 5.2 ($CH_2CH_2$), 29.8 (d, $^2J_{C\text{-}P}$ = 16.0 Hz, $CHCH_2$), 41.8 (d, $^1J_{C\text{-}P}$ = 136.1 Hz, P*C*H), 55.2 ($OCH_3$), 55.4 ($OCH_3$), 66.5 (d, $^2J_{C\text{-}P}$ = 6.7 Hz, $CH_2CH_3$), 66.8 (d, $^2J_{C\text{-}P}$ = 6.8 Hz, $CH_2CH_3$), 76.6 ($PhCH_2$), 111.6, 112.7 (d, $^3J_{C\text{-}P}$ = 6.3 Hz), 121.3 (d, $^3J_{C\text{-}P}$ = 7.3 Hz), 127.4, 127.5, 127.6, 128.0, 128.1, 128.2, 128.2, 128.4,

128.6, 136.0, 136.5 (d, $^3J_{C\text{-}P}$ = 6.4 Hz), 136.6 (d, $^3J_{C\text{-}P}$ = 6.0 Hz), 147.9 (d, $^5J_{C\text{-}P}$ = 2.5 Hz), 148.4, 168.47 (*C*=O) ppm; anal. calcd. for $C_{33}H_{36}NO_7P$: C 67.22, H 6.15, N 2.38, found: C 67.47, H 6.27, N 2.36.

**General procedure for the synthesis of carboxylic acid 20, hydroxamic acid 22, *o*-hydroxyanilide 31, bisphosphonate 7 and target compounds 2a-f, 3b and 4.**[29] To a solution of the appropriate *O*-Bn-protected hydroxamic acid (1 mmol) in freshly distilled methanol (20 mL), Pd-C catalyst (10 %, 40 mg) was added. The mixture was hydrogenated for 1 h (in case of compounds **2a**, **2c**, **4**, **20**, **22**, **31**) and 3 h (in case of compounds **2b**, **2d-f**, **3b**, **7**). The catalyst was removed by filtration and the solvent was evaporated under reduced pressure. Pure target compounds **2b** and **2d-f** were obtained as white solids after addition of ethyl acetate. Recrystallization in ethyl acetate gave compound **31** as colorless crystals. Pure compounds **2a**, **2c**, **3b**, **4**, **7**, **20** and **22** were obtained without further purification.

**1-(3,4-Dimethoxyphenyl)-4-[hydroxy(methyl)amino]-4-oxobutylphosphonic acid (2e).** White solid (290 mg, 87 %) mp: 70 °C; $^1$H NMR (500.13 MHz, [D6]DMSO): δ = 1.89-1.99 (m, 1H, C$H_2$), 2.19 (s, 3H, C$H_2$), 2.77-2.84 (m, 1H, PC*H*), 3.03 (s, 3H, NC$H_3$), 3.71 (s, 3H, OC$H_3$), 3.72 (s, 3H, OC$H_3$), 6.74-6.76 (m, 1H), 6.85-6.87 (m, 2H), 9.68 (br s, 1H, O*H*) ppm; $^{13}$C NMR (125.76 MHz, [D6]DMSO): δ = 25.3 ($CH_2CH_2$), 30.1 (d, $^2J_{C\text{-}P}$ = 15.2 Hz, $CHCH_2$), 35.6 ($NCH_3$), 44.1 (d, $^1J_{C\text{-}P}$ = 136.8 Hz, P*C*H), 55.3 ($OCH_3$), 55.45 ($OCH_3$), 111.6, 112.8 (d, $^3J_{C\text{-}P}$ = 5.6 Hz), 121.3 (d, $^2J_{C\text{-}P}$ = 7.2 Hz), 130.5 (d, $^3J_{C\text{-}P}$ = 6.5 Hz), 147.3, 148.3, 172.7 (*C*=O) ppm; anal. calcd. for $C_{13}H_{20}NO_7P$: C 46.85, H 6.05, N 4.20, found: C 46.61, H 6.05, N 4.06.

**1-(3,4-Dimethoxyphenyl)-4-(hydroxyamino)-4-oxobutylphosphonic acid (2f).** White solid (313 mg, 98 %), mp: 75 °C; $^1$H NMR (500.13 MHz, [D6]DMSO): δ = 1.73-1.93 (m, 3H, C$H_2$), 2.20-2.28 (m, 1H, C$H_2$), 2.75 (ddd, *J* = 14.9, 10.9, 3.5 Hz, 1H, PC*H*), 3.72 (s, 6H, OC$H_3$), 6.75-6.76 (m, 1H), 6.84-6.87 (m, 2H), 8.66 (br s, 1H, OH), 9.71 (s, 0.1H, *E*-isomer, N*H*), 10.27 (s, 0.9H, *Z*-isomer, N*H*) ppm; $^{13}$C NMR (125.76 MHz, [D6]DMSO): δ = 26.4 ($CH_2CH_2$), 30.6 (d, $^2J_{C\text{-}P}$ = 15.2 Hz, $CHCH_2$), 44.2 (d, $^1J_{C\text{-}P}$ = 134.6 Hz, P*C*H), 55.3 ($OCH_3$), 55.4 ($OCH_3$), 111.6, 112.8 (d, $^3J_{C\text{-}P}$ = 6.2 Hz), 121.1 (d, $^3J_{C\text{-}P}$ = 6.7 Hz),

130.5 (d, $^{2}J_{C\text{-}P}$ = 6.4 Hz), 147.3 (O*C*$H_3$), 148.2 (O*C*$H_3$), 168.8 (*C*=O) ppm; HPLC analysis: retention time = 1.54 min; peak area: 97.5 %. Eluent A: 5 mM $NH_4OAc$ solution; eluent B: $CH_3CN$, isocratic (1:1) over 20 min at a flow rate of 1.5 mL $min^{-1}$.

## ASSOCIATED CONTENT

**Supporting Information.** Experimental procedures, analytical data, enzyme assays, biological evaluation of *in vitro* antiplasmodial activity, and experimental data regarding crystallization and structure determination. This material is available free of charge via the Internet at http://pubs.acs.org.

## AUTHOR INFORMATION

**Corresponding Author**

*Phone: (+49)21181-14984. Fax: (+49)22181-13847. E-mail: Thomas.kurz@uni-duesseldorf.de.

## ACKNOWLEDGMENT

Nobutada Tanaka was supported in part by a grant from the Takeda Science Foundation, the Naito Foundation, and Grant-in-Aid for Scientific Research (C) from the MEXT of Japan.

We are very grateful for the support by the Hans-Fischer-Gesellschaft and the Deutsche Forschungsgemeinschaft, grant GR 3866/1-1.

## ABBREVIATIONS

*n*-BuLi, *n*-butyllithium; CDI, 1,1`-carbonyldiimidazol; DCC, *N,N`*-dicyclohexylcarbodiimide; DMF, *N,N*-dimethylformamide; DMSO, dimethyl sulfoxide; DOXP, 1-deoxy-D-xylulose 5-phosphate; Dxr (IspC), 1-deoxy-D-xylulose 5-phosphate reductoisomerase; MEP, 2*C*-methyl-D-erythritol 4-phosphate; NADPH, nicotinamide adenine dinucleotide phosphate; NMM, *N*-methymorpholine; Pd-C, palladium on activated carbon; rt, room temperature; TEA, triethylamine; THF, tetrahydrofurane; TMSBr, bromotrimethylsilane; WHO, World Health Organization.

## REFERENCES

1) http://www.who.int/malaria/publications/world_malaria_report_2013/wmr2013_no_profiles.pdf?ua=1

2) Rodriguez-Concepcion, M., The MEP pathway: a new target for the development of herbicides, antibiotics and antimalarial drugs. *Curr Pharm Des* **2004**, *10* (19), 2391-2400.

3) Dondorp, A. M.; Nosten, F.; Yi, P.; Das, D.; Phyo, A. P.; Tarning, J.; Lwin, K. M.; Ariey, F.; Hanpithakpong, W.; Lee, S. J.; Ringwald, P.; Silamut, K.; Imwong, M.; Chotivanich, K.; Lim, P.; Herdman, T.; An, S. S.; Yeung, S.; Singhasivanon, P.; Day, N. P. J.; Lindegardh, N.; Socheat, D.; White, N. J. Artemisinin Resistance in *Plasmodium falciparum* Malaria. *N. Engl. J. Med.* **2009**, *361* (5), 455-467.

4) Kuroda, Y.; Okuhara, M.; Goto, T.; Okamoto, M.; Terano, H.; Kohsaka, M.; Aoki, H.; Imanaka, H. Studies on new phosphonic acid antibiotics. IV. Structure determination of FR-33289, FR-31564 and FR-32863. *J Antibiot (Tokyo)* **1980**, *33* (1), 29-35.

5) Koppisch, A. T.; Fox, D. T.; Blagg, B. S. J.; Poulter, C. D. E-coli MEP synthase: Steady-state kinetic analysis and substrate binding. *Biochemistry* **2002**, *41* (1), 236-243.

6) Rohmer, M.; Knani, M.; Simonin, P.; Sutter, B.; Sahm, H. Isoprenoid biosynthesis in bacteria: a novel pathway for the early steps leading to isopentenyl diphosphate. *Biochem J* **1993**, *295 ( Pt 2)*, 517-524.

7) Rohmer, M.; Grosdemange-Billiard, C.; Seemann, M.; Tritsch, D. Isoprenoid biosynthesis as a novel target for antibacterial and antiparasitic drugs. *Curr. Opin. Invest. Drugs* **2004**, *5*, 154−162.

8) Rohdich, F.; Bacher, A.; Eisenreich, W. Isoprenoid biosynthetic pathways as anti-infective drug targets. *Biochem. Soc. Trans.* **2005**, *33*, 785−791.

9) Okuhara, M.; Kuroda, Y.; Okamoto, M.; Terano, H.; Kohsaka, M.; Aoki, H. Imanaka, H. Studies on new phosphonic acid antibiotics. 3. Isolation and characterization of FR-31564, FR-32863 and FR-33289. *J. Antibiot.* **1980**, *33*, 24-28.

10) Jomaa, H.; Wiesner, J.; Sanderbrand, S.; Altincicek, B.; Weidemeyer, C.; Hintz, M.; Turbachova, I.; Eberl, M.; Zeidler, J.; Lichtenthaler, H. K.; Soldati, D.; Beck, E. Inhibitors of the nonmevalonate pathway of isoprenoid biosynthesis as antimalarial drugs. *Science* **1999**, *285* (5433), 1573-1576.

11) Borrmann, S.; Lundgren, I.; Oyakhirome, S.; Impouma, B.; Matsiegui, P.-B.; Adegnika, A. A.; Issofou, S.; Kun, J. F. J.; Hutchinson, D.; Wiesner, J.; Jomaa, H.; Kremsner, P.G. Fosmidomycin plus Clindamycin for Treatment of Pediatric Patients Aged 1 to 14 Years with *Plasmodium falciparum* Malaria. *Antimicrob. Agents and Chemother.* **2006**, *50* (8), 2713-2718.

12) Oyakhirome, S.; Issifou, S.; Pongratz, P; Barondi, F.; Ramharter, M.; Kun, J. F.; Missinou, M. A.; Lell, B.; Kremsner, P. G. Randomized Controlled Trial of Fosmidomycin-Clindamycin versus Sulfadoxine-Pyrimethamine in the Treatment of *Plasmodium falciparum* Malaria. *Antimicrob. Agents and Chemother.* **2007**, *51* (5), 1869-1871.

13) Na-Bangshang, K.; Ruengweerayut, R.; Karbwang, J.; Chauemung, A.; Hutchinson, D. Pharmacokinetics and pharmacodynamics of fosmidomycin monotherapy and combination therapy with clindamycin in the treatment of multidrug resistant falciparum malaria. *Malaria Journal* **2007**, *6*, 1-10.

14) Kunfermann, A.; Lienau, C.; Illarionov, B.; Held, J.; Gräwert, T.; Behrendt, C.; Werner, P.; Hähn, S.; Eisenreich, W.; Riederer, U.; Mordmüller, B.; Bacher, A.; Fischer, M.; Groll, M.; Kurz, T. IspC as Target for Antiinfective Drug Discovery: Synthesis, Enantiomeric Separation, and Structural Biology of Fosmidomycin Thia Isosters. *J. Med. Chem.* **2013**, *56*, 8151-8162.

15) Umeda, T.; Tanaka, N.; Kusakabe, Y.; Nakanishi, M.; Kitade, Y.; Nakamura, K. T. Molecular basis of fosmidomycin's action on the human malaria parasite *Plasmodium falciparum*. *Sci. Rep.*, **2011**, *1*, article number 9.

16) Xue, J.; Diao, J.; Cai, G.; Deng, L.; Zheng, B.; Yao, Y.; Song, Y. Antimalarial and Structural Studies of Pyridine-Containing Inhibitors of 1-Deoxyxylulose-5-phosphate Reductoisomerase. *ACS Med. Chem. Lett.* **2013**, *4*, 278-282.

17) Behrendt, C. T.; Kunfermann, A.; Illarionova, V.; Matheeussen, A.; Pein, M. K.; Gräwert, T.; Kaiser, J.; Bacher, A.; Eisenreich, W.; Illarionov, B.; Fischer, M.; Maes, L.; Groll, M.; Kurz, T. Reverse Fosmidomycin Derivatives against the Antimalarial Drug Target IspC (Dxr). *J. Med. Chem.* **2011**, *54*, 6796-6802.

18) Reuter, K.; Sanderbrand, S.; Jomaa, H.; Wiesner, J.; Steinbrecher, I.; Beck, E.; Hintz, M.; Klebe, G.; Stubbs, M. T. Crystal Structure of 1-Deoxy-d-xylulose-5-phosphate Reductoisomerase, a Crucial Enzyme in the Non-mevalonate Pathway of Isoprenoid Biosynthesis. *J. Biol. Chem.* **2002**, *277*, 5378-5384.

19) Yajima, S.; Hara, K.; Sanders, J. M.; Yin, F.; Ohsawa, K.; Wiesner, J.; Jomaa, H.; Oldfield, E. Crystallographic structures of two bisphosphonate:1-deoxyxylulose-5-phosphate reductoisomerase complexes. *J. Am. Chem. Soc.* **2004**, *126*, 10824−10825.

20) Deng, L.; Endo, K.; Kato, M.; Cheng, G.; Yajima, S.; Song, Y. Structures of 1-deoxy-D-xylulose-5-phosphate reductoisomerase/lipophilic phosphonate complexes. *ACS Med. Chem. Lett.* **2011**, *2*, 165−170.

21) Yajima, S.; Nonaka, T.; Kuzuyama, T.; Seto, H.; Ohsawa, K. Crystal structure of 1-deoxy-D-xylulose 5-phosphate reductoisomerase complexed with cofactors: Implications of a flexible loop movement upon substrate binding. *J. Biochem.* **2002**, *131*, 313−317.

22) Steinbacher, S.; Kaiser, J.; Eisenreich, W.; Huber, R.; Bacher, A.; Rohdich, F. Structural basis of fosmidomycin action revealed by the complex with 2-C-methyl-D-erythritol 4-phosphate synthase (IspC). Implications for the catalytic mechanism and anti-malaria drug development. *J. Biol. Chem.* **2003**, *278*, 18401.

23) Mac Sweeney, A.; Lange, R.; Fernandes, R. P.; Schulz, H.; Dale, G. E.; Douangamath, A.; Proteau, P. J.; Oefner, C. The crystal structure of E.coli 1-deoxy-D-xylulose-5-phosphate

reductoisomerase in a ternary complex with the antimalarial compound fosmidomycin and NADPH reveals a tight-binding closed enzyme conformation. *J. Mol. Biol.* **2005**, *345*, 115−127.

24) Yajima, S.; Hara, K.; Iino, D.; Sasaki, Y.; Kuzuyama, T.; Ohsawa, K.; Seto, H. Structure of 1-deoxy-D-xylulose 5-phosphate reductoisomerase in a quaternary complex with a magnesium ion, NADPH and the antimalarial drug fosmidomycin. Acta Crystallogr., Sect. F: Struct. Biol. Cryst. Commun. 2007, 63, 466−470.

25) Jansson, A. M.; Więckowska, A.; Björkelid, C.; Yahiaoui, S.; Sooriyaarachchi, S.; Lindh, M.; Bergfors, T.; Dharavath, S.; Desroses, M.; Suresh, S.; Andaloussi, M.; Nikhil, R.; Sreevalli, S.; Srinivasa, B. R.; Larhed, M.; Jones, T. A.; Karlén, A.; Mowbray, S. L. DXR Inhibition by Potent Mono- and Disubstituted Fosmidomycin Analogues. *J. Med. Chem.* **2013**, *56*, 6190-6199.7

26) Andaloussi, M.; Henriksson, L. M.; Wieckowska, A.; Lindh, M.; Bjorkelid, C.; Larsson, A. M.; Suresh, S.; Iyer, H.; Srinivasa, B. R.; Bergfors, T.; Unge, T.; Mowbray, S. L.; Larhed, M.; Jones, T. A.;Karlén, A. Design, synthesis, and X-ray crystallographic studies of α-aryl substituted fosmidomycin analogues as inhibitors of Mycobacterium tuberculosis 1-deoxy-D-xylulose 5-phosphate reductoisomerase. *J. Med. Chem.* **2011**, *54*, 4964-4976.

27) Deng, L.; Diao, J.; Chen, P.; Pujari, V.; Yao, Y.; Chemg, G.; Crick, D. C.; Prasad, B. V. V.; Song, Y. Inhibition of 1-deoxy-D-xylulose 5-phosphate reductoisomerase by lipophilic phosphonates: SAR, QSAR, and crystallographic studies. *J. Med. Chem.* **2011**, *54*, 4721-4734.

28) Henriksson, L. M.; Unge, T.; Carlsson, J.; Aqvist, J.; Mowbray, S. L.; Jones, T. A. Structures of Mycobacterium tuberculosis 1-Deoxy-D-xylulose-5-phosphate Reductoisomerase Provide New Insights into Catalysis. *J. Biol. Chem.* **2007**, *282*, 19905-19916.

29) Behrendt, C. T.; Kunfermann, A.; Illarionova, V.; Matheeussen, A.; Gräwert, T.; Groll, M.; Rohdich, F.; Bacher, A.; Eisenreich, W.; Fischer, M.; Maes, L.; Kurz, T. Synthesis and Antiplasmodial Activity of Highly Active Reverse Analogues of the Antimalarial Drug Candidate Fosmidomycin. *ChemMedChem* **2010**, *5*, 1673-1676.

30) Brücher, K.; Illarionov, B.; Held, J.; Tschan, S.; Kunfermann, A.; Pein, M. K.; Bacher, A.; Gräwert, T.; Maes, L.; Mordmüller, B.; Fischer, M.; Kurz, T. α-Substituted β-Oxa Isosteres of Fosmidomycin: Synthesis and Biological Evaluation. *J. Med. Chem.* **2012**, *55*, 6566-6575.

31) Hirano, H.; Osawa, E.; Yamaoka, Y.; Yokoi, T. Gastric-Mucous Membrane Protection Activity of Coptisine Derivatives. *Biol. Pharm. Bull.* **2001**, *24*, 1277-1281.

32) De Macedo Puyau, P.; Perie, J. J. Synthesis of Substrate Analogues and Inhibitors for the Phosphoglycerate Mutase Enzyme. *Phosphorus, Sulphur, and Silicon.* **1997**, *129*, 13-45.

33) Shendage, D. M.; Fröhlich, R.; Haufe, G. Highly Efficient Stereoconservative Amidation and Deaminationof α-Amino Acids. *Org. Lett.* **2004**, *6*, 3675-3678.

34) Vugts, D. J.; Koningstein, M. M.; Schmitz, R. F.; De Canter, F. J. J.; Groen, M. B.; Orru, R. V. A. Multicomponent Synthesis of Dihydropyrimidines and Thiazines. *Chem. Eur. J.* **2006**, *12*, 7178-7189.

35) Varseev, G. N.; Maier, M. E. A Novel Palladium-Catalyzed Arylation-Dehydroaromatization Reaction: Synthesis of 7-Aryltetralones. *Org. Lett.* **2005**, *7*, *18*, 3881-3884.

36) Diel, P. J.; Maier, L. Organische Phosphorverbindungen 79[1] Herstellung und Eigenschaften von α-Amino-ω-Carboxyalkylphosphon- und Phosphinsäuren. *Phosphorus and Sulfur* **1987**, *29*, 201-209.

37) Neelarapu, R.; Holzle, D. L.; Velaparthi, S.; Bai, H.; Brunsteiner, M.; Blond, S. Y.; Petukhov, P. A. Design, Synthesis, Docking, and Biological Evaluation of Novel Diazide-Containing Isoxazole- and Pyrazole-Based Histone Deacetylase Probes. *J. Med. Chem.* **2011**, *54*, 4350-4364.

38) Aspinall, H. C.; Greeves, N.; McIver, E. G. Modular chiral polyether podands and their lanthanide complexes. *Tetrahedron* **2003**, *59*, 10453-10463.

39) Kuzmic, P. Program DYNAFIT for the analysis of enzyme kinetic data; Application to HIV proteinase. *Anal. Biochem.* **1996**, *237*,260-273.

40) Noedl, H.; Bronnert, J.; Yingyuen, K.; Attlmayr, B.; Kollaritsch, H.; Fukuda, M. Simple Histidine-Rich Protein 2 Double-Site Sandwich Enzyme-Linked Immunosorbent Assay for Use in Malaria Drug Sensitivity Testing. *Antimicrob. Agents Chemother.* **2005**, *49*, 3575-3577.

41) Press, W. H.; Teukolsky, S. A.; Vetterling, W. T.; Flannery, B. P. Numerical Recipes: The Art of Scientific Computing, 3rd ed.; Cambridge University Press: New York, 2007; Chapter 15; pp 773-774 and pp 788-816.

42) Kuntz, L.; Tritsch, D.; Grosdemange-Billiard, C.; Hemmerlin, A.; Willem, A.; Bach, T. J.; Rohmer, M. Isopreonoid biosynthesis as a target for antibacterial and antiparasitic drugs: phosphonohydroxamic acids as inhibitors of deoxyxylulose phosphate reductoisomerase. *Biochem. J.* **2005**, *386*, 127-135.

43) Haemers, T.; Wiesner, J.; Busson, R.; Jomaa, H.; Van Calenbergh, S. Synthesis of α-aryl-substituted and conformationally restricted fosmidomycin analogues as promising antimalarials. *Eur. J. Org. Chem.* **2006**, 3856−3863.

TABLE OF CONTENTS GRAPHIC